1985

Slow crack growth due to temperature change /

Chich-Kuan Chen
Lehigh University

SLOW CRACK GROWTH DUE TO TEMPERATURE CHANGE

by

Chich-Kuan Chen

A Thesis

Presented to the Graduate Committee

of Lehigh University

in Candidacy for the Degree of

Master of Science

in

Applied Mechanics

Lehigh University

1985

This thesis is accepted and approved in partial fulfillment of the requirements for the degree of Master of Science.

September 16, 1985
(date)

Professor in Charge

Chairman of Department

ACKNOWLEDGEMENTS

The author would like to thank Professor G. C. Sih for his guidance and encouragement which made this work possible. The input of his graduate students in the Institute of Fracture and Solid Mechanics is also gratefully acknowledged.

Thanks are also due to Mrs. Barbara DeLazaro and Mrs. Connie Weaver for their care and assistance.

Special thanks are to my dearest parents and brother for their unfailing love to me while I was away from home.

TABLE OF CONTENTS

CERTIFICATE OF APPROVAL		ii
ACKNOWLEDGEMENT		iii
TABLE OF CONTENTS		iv
LIST OF TABLES		vi
LIST OF FIGURES		vii
ABSTRACT		1
CHAPTER 1:	INTRODUCTION	3
CHAPTER 2:	STRAIN ENERGY DENSITY CRITERION	5
	2.1 Strain Energy Density Function	5
	2.2 Hypotheses	8
	2.3 Onset of Global Instability	9
CHAPTER 3:	FINITE ELEMENT FORMULATION	10
	3.1 General Remarks	10
	3.2 Displacement Expression	11
	3.3 Uncoupled Linear Isotropic Thermal Elasticity	13
	3.4 Finite Element Analysis	14
	3.4.1 Heat Conduction	14
	3.4.2 Stress Distribution	14
CHAPTER 4:	TEMPERATURE FIELD AND CRACK GROWTH	16
	4.1 Material Properties	16
	4.2 Geometric Configuration and Boundary Conditions	17
	4.3 Temperature Rise on Crack Surface	21
	4.4 Partially Insulated Crack	30

TABLE OF CONTENTS - (CONTINUED)

CHAPTER 5:	CRACK GROWTH RESISTANCE CURVES	40
CHAPTER 6:	CONCLUSIONS AND RECOMMENDATION FOR FUTURE RESEARCH	44
REFERENCES		48
VITA		50

LIST OF TABLES

Table 1 - Crack growth data for temperature specified on crack surface. 22

Table 2 - Crack growth data for a partially insulated crack. 31

LIST OF FIGURES

Figure 1 - Schematic of a volume element ahead of crack. 6

Figure 2 - Strain energy density versus polar angle: distortion and dilatation. 7

Figure 3 - Coordinate mapping for 12-nodes isoparametric element. 12

Figure 4 - Configuration of centrally cracked panel. 18

Figure 5 - Triangular finite element grid pattern used in heat conduction. 19

Figure 6 - Finite element grid pattern used in stress analysis. 20

Figure 7 - Constant temperature contours for crack with surface temperature rise - crack growth step no. 6. 23

Figure 8 - Variation of dW/dV versus distance for crack growth, step no. 1 with equation (13) as boundary condition. 24

Figure 9 - Variation of dW/dV versus distance for crack growth, step no. 2 with equation (13) as boundary condition. 25

Figure 10 - Variation of dW/dV versus distance for crack growth, step no. 3 with equation (13) as boundary condition. 26

Figure 11 - Variation of dW/dV versus distance for crack growth, step no. 4 with equation (13) as boundary condition. 27

Figure 12 - Variation of dW/dV versus distance for crack growth, step no. 5 with equation (13) as boundary condition. 28

Figure 13 - Variation of dW/dV versus distance for crack growth, step no. 6 with equation (13) as boundary condition. 29

Figure 14 - Contours of constant temperature for a partially insulated crack after four steps of growth. 32

LIST OF FIGURES - (CONTINUED)

Figure 15 - Variation of dW/dV versus distance for crack growth, step no. 1 with equation (14) as boundary condition. 33

Figure 16 - Variation of dW/dV versus distance for crack growth, step no. 2 with equation (14) as boundary condition. 34

Figure 17 - Variation of dW/dV versus distance for crack growth, step no. 3 with equation (14) as boundary condition. 35

Figure 18 - Variation of dW/dV versus distance for crack growth, step no. 4 with equation (14) as boundary condition. 36

Figure 19 - Variation of dW/dV versus distance for crack growth, step no. 5 with equation (14) as boundary condition. 37

Figure 20 - Variation of dW/dV versus distance for crack growth, step no. 6 with equation (14) as boundary condition. 38

Figure 21 - R-curve for crack with increasing surface temperature. 41

Figure 22 - R-curve for crack with partially insulated surface. 42

Figure 23 - Crack growth as a function of temperature on crack surface. 45

Figure 24 - Crack growth as a function of temperature on panel edge. 46

ABSTRACT

It is generally recognized that metal fails by a process of excessive deformation and fracture. Cracks are initiated and then spread slowly prior to final termination. This physical process can be conveniently and consistently modeled by application of the strain energy criterion.

One of the major research topics in fracture mechanics is determining the crack resistance that varies as a function of crack growth. The high nonlinear variations of the applied load with crack growth cannot be readily used in engineering applications because they are too sensitive to changes in loading rate, specimen size and geometry and other design variables. Clearly, the objective is to seek a suitable parameter whose variations with crack growth can be predetermined so as to provide information for situations other than those tested. Otherwise, the crack-extension resistance curves can serve little or no useful purpose.

The strain energy density failure criterion is applied to the steady state, thermoelastic problem involving cracks in regions of finite dimensions. Assumed is that failure can be uniquely associated with the rate at which energy is dissipated in a unit volume of material. This quantity shall be referred to as the strain energy density function dW/dV, whose critical value $(dW/dV)_c$ corresponds to certain threshold levels of material damage. The amount of energy released through a small distance r can be measured by the strain energy den-

sity factor defined as S = r(dW/dV). Such a relation remains valid for all materials as S is not limited to the type of constitutive relations used.

The present work is concerned with linear thermoelastic stress and failure analysis of a centrally cracked panel subject to thermal loading. Two types of boundary conditions are considered. One deals with the step rise of surface temperature on crack and the other with temperature rise on the specimen edges while the crack is partially insulated from heat transfer. Crack growth resistance curves are obtained by plotting S as a function of half crack length. These curves are straight lines satisfying the condition dS/da = const. The straight line relation of S versus a is particularly useful to the designers who can extrapolate the data for use in situations other than those analyzed.

CHAPTER 1: INTRODUCTION

The main requirement of a well-designed structure is its loading carrying capacity over the specified life span. The stress and strain induced by different loads will depend on the geometry and size and material properties of the structural member. Geometric discontinuities such as re-entrant corners, notches, cracks and other defects can result in local stresses many times higher than those at distances further away. Th se localized stress concentrations can have a significant influence on the load bearing capacity of structural components. Failure can occur in the form of yielding due to excessive shape change, fracture due to excessive volume change, or a combination of the two.

All material, however, contain inherent mechanical imperfections which may spread under appropriate loading conditions. Material behavior can change in time because of periodic damage that is cumulative in nature. It is, therefore, essential to develop the means of predicting material damage as a function of loading history, component size and shape and material type for a given environment. Such an attempt is being made currently by researchers in the Institute of Fracture and Solid Mechanics at Lehigh University.

The basic philosophy of continuum mechanics is that the material properties of a solid can be evaluated experimentally from uniaxial tensile or compressive tests. In the case of linear elasticity, this procedure is accomplished by introducing the concept of superposition.

This necessitates an additional parameter known as the Poisson's ratio. Since elasticity does not address material damage, failure criterion must be invoked. The strain energy density criterion [1-5] is suited for analyzing subcritical crack growth accompanied by reversible or irreversible deformation, mainly because it can treat the initiation, slow growth and termination of the fracture process in a consistent and unique fashion. No limitations are imposed on non self-similar crack growth nor on dimensionality of the crack configuration. The criterion can also account for change in resistance to crack growth when yielding of varying degrees occur along the prospective crack path.

Considered in this work is the finite element formulation of thermoelastic problems with cracks. The strain energy density criterion is applied to determine the incremental growth of a single crack as the temperature change is increased in steps. The variation of the strain energy factor with crack growth is found to follow a straight line relationship that can be easily used for assessing thickness and/or loading rate effects. Even for linear elastic problems, where no plasticity prevails, slow crack growth is still affected by the load-time history [6].

CHAPTER 2: STRAIN ENERGY DENSITY CRITERION

2.1 Strain Energy Density Function

When a solid is loaded, there prevails a nonuniform distribution of energy in terms of the space and time variable. In the presence of a preexisting crack, the energy per unit volume ahead of the crack can be elevated sufficiently high to initiate crack growth. This is illustrated schematically in Figure 1. A core region with radius r_o is normally defined to observe the scale level at which the analysis is being made. Hence, the so-called strain energy function, dW/dV, nearest to the crack tip is determined outside of this region.

In general, the strain energy density function can be computed from

$$\frac{dW}{dV} = \int_0^{\varepsilon_{ij}} \sigma_{ij} d\varepsilon_{ij} + F(\Delta C, \Delta T) \qquad (1)$$

with ΔT and ΔC being changes in temperature and moisture concentration. The stress and strain components are denoted by σ_{ij} and ε_{ij}, respectively. With reference to the crack for a fixed distance r in Figure 1 or Figure 2, dW/dV will vary as a function of the polar angle θ. There prevails a relative maximum $(dW/dV)_{max}$ and a relative minimum $(dW/dV)_{min}$. The former can be associated with yield initiation and the latter with fracture initiation [1].

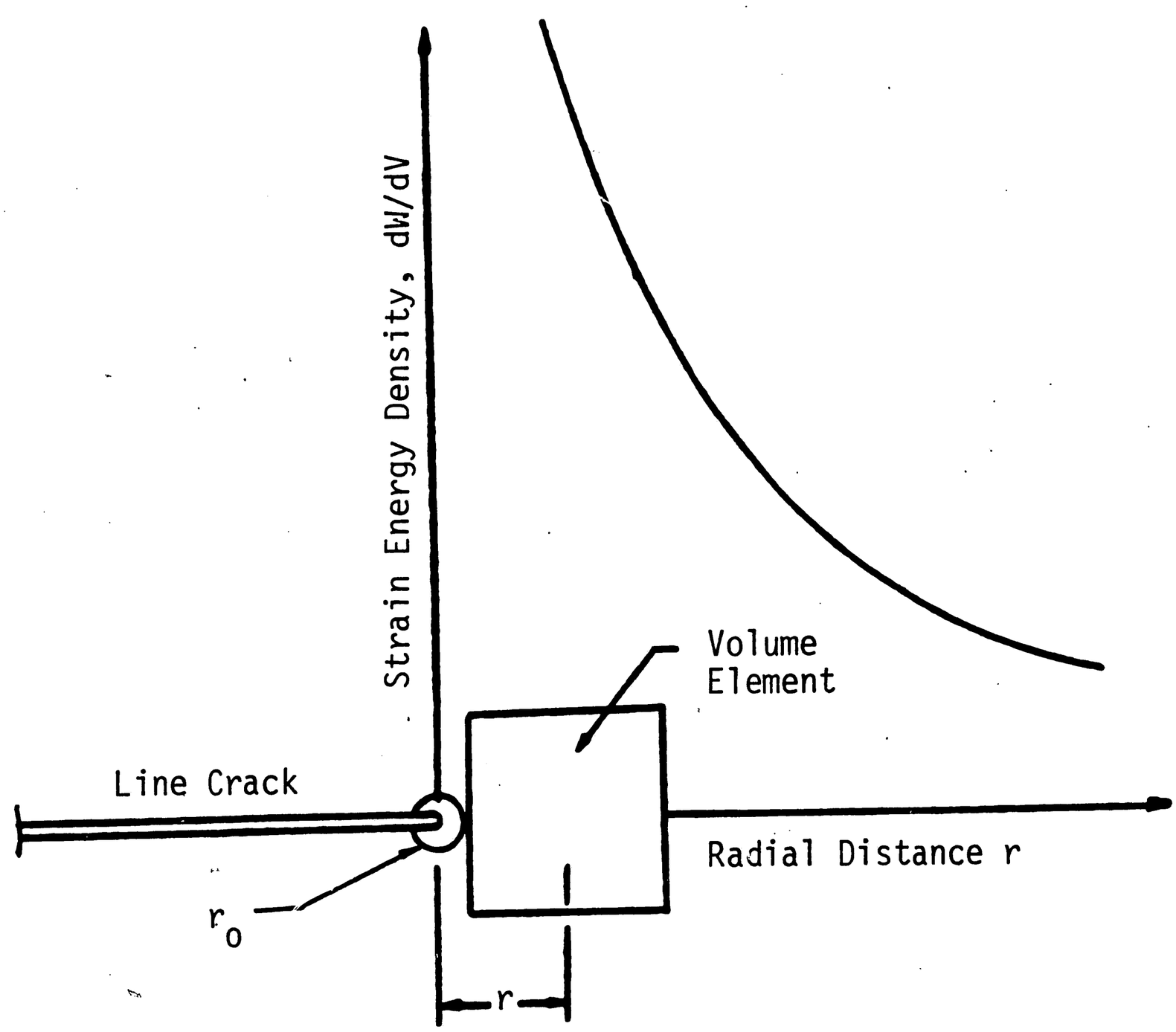

Figure 1 - Schematic of a volume element ahead of crack.

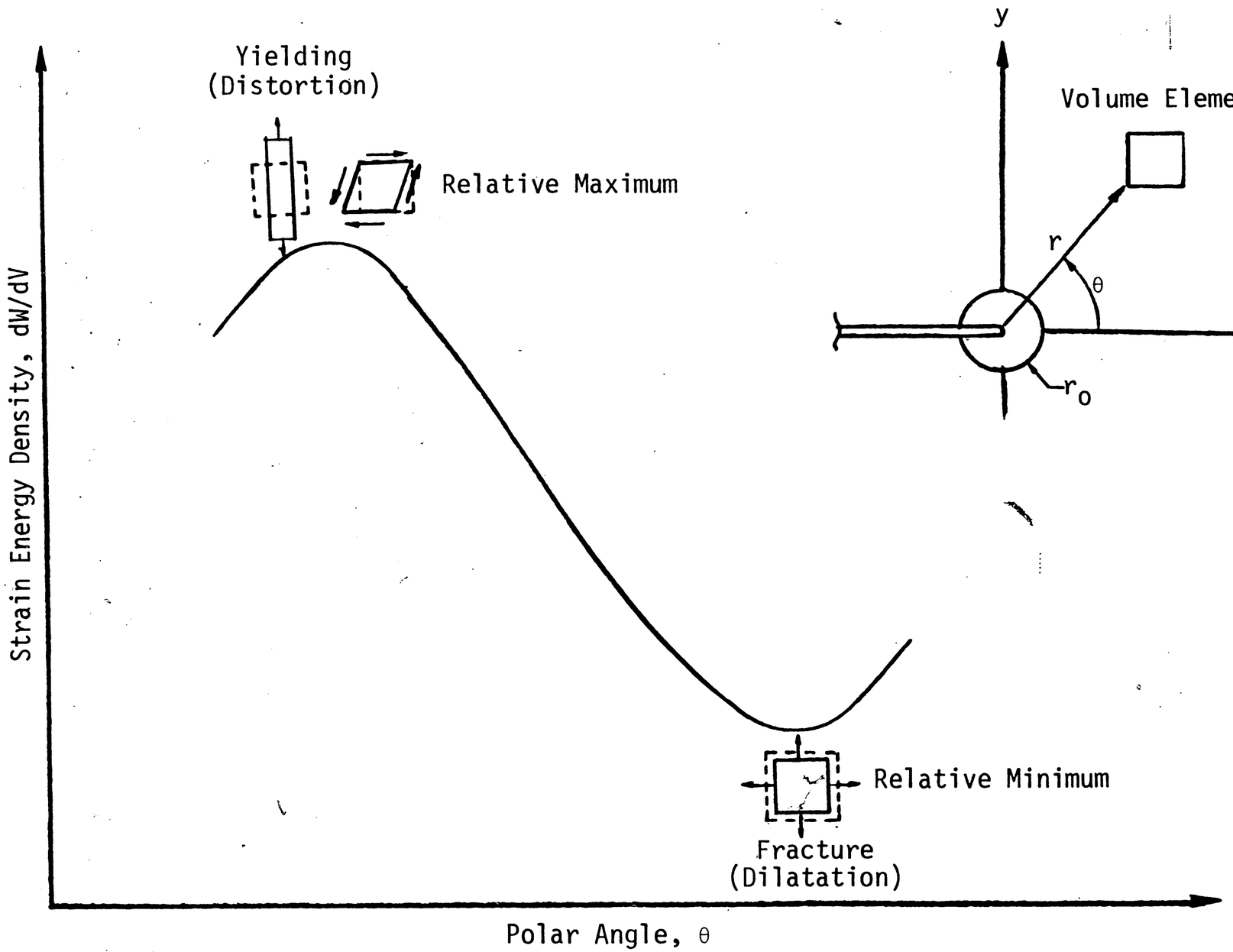

Figure 2 - Strain energy density versus polar angle: distortion and dilatation.

RETAKE

The Operator has Determined that the Previous Frame is Unacceptable and Has Refilmed the Page in the Next Frame.

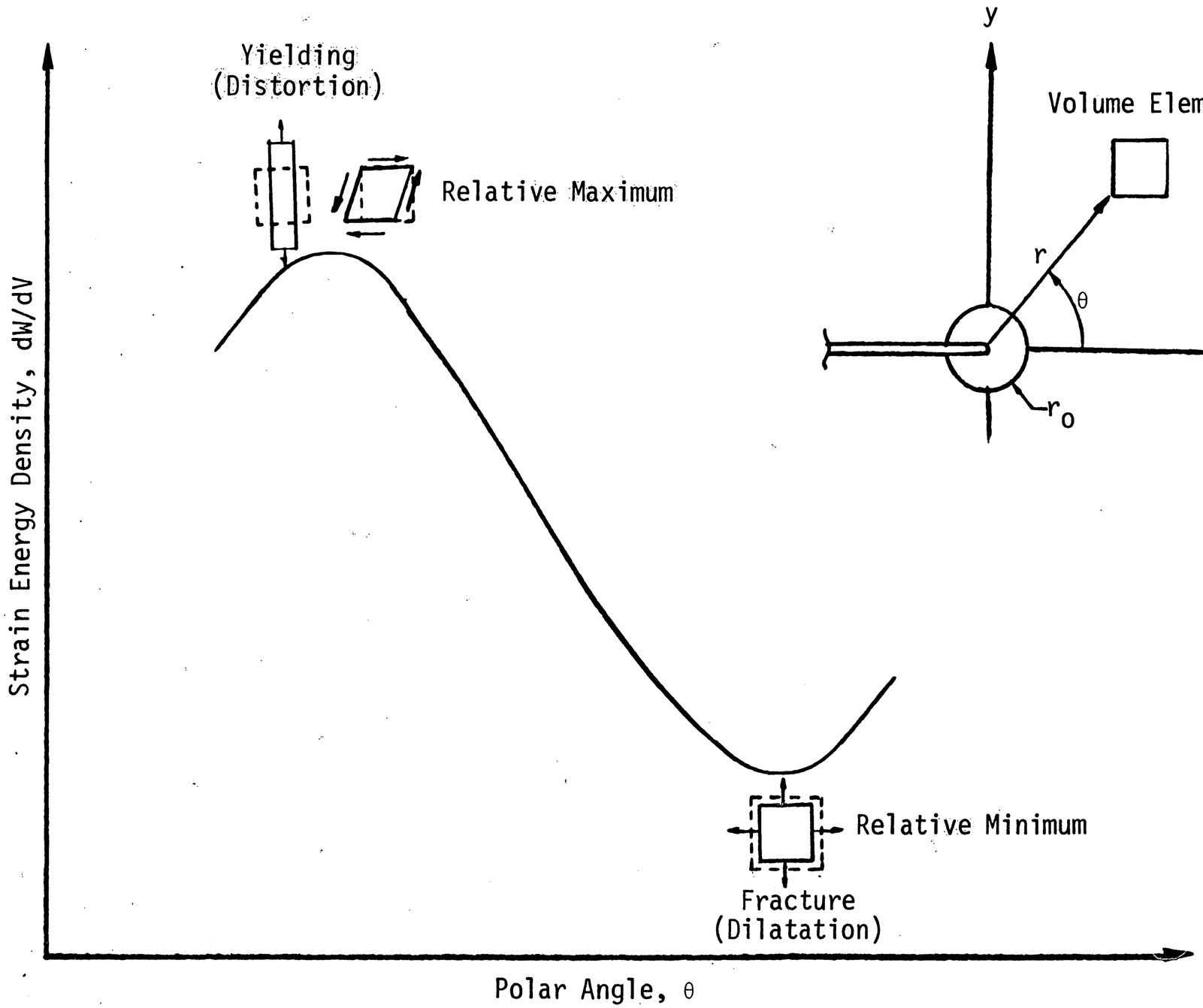

Figure 2 - Strain energy density versus polar angle: distortion and dilatation.

2.2 Hypotheses

The strain energy density criterion may be stated in terms of three fundamental hypotheses and it applies to all structure geometries, loading type and material with or without initial flaw.

1. The relative local and global minima of dW/dV or $(dW/dV)_{min}$ and maxima of dW/dV, $(dW/dV)_{max}$, are assumed to coincide with the locations of fracture and yielding, respectively.

2. Yielding and fracture are assumed to occur when the maximum of $(dW/dV)_{max}$ or $(dW/dV)_{min}$ reach their respective critical values.

3. The rate of yielding and fracture are assumed to obey the relation

$$\left(\frac{dW}{dV}\right)_c = \frac{S_1}{r_1} = \frac{S_2}{r_2} = \text{---} = \frac{S_j}{r_j} = \text{---} = \frac{S_c}{r_c} \text{ or } \frac{S_o}{r_o} < \left(\frac{dW}{dV}\right)_c \qquad (2)$$

If the process leads to global instability, then the inequalities

$$S_1 < S_2 < \text{---} < S_j < \text{---} < S_c \qquad (3)$$

$$r_1 < r_2 < \text{---} < r_j < \text{---} < r_c$$

will hold. In situations where yielding and fracture come

to arrest, the following shall apply:

$$S_1 > S_2 > \text{---} > S_j > \text{---} > S_o$$
$$r_1 > r_2 > \text{---} > r_j > \text{---} > r_o \qquad (4)$$

For a linear elastic material, tested to failure under uniaxial loading, $(dW/dV)_c$ is simply equal to $\sigma_{yd}^2/2E$ where σ_{yd} is the yield strength and E the Young's modulus.

2.3 Onset of Global Instability

This event can occur catastrophically or less dramatic depending on the *rate of energy* released during the breakage of the last ligament of material. If the release involves predominantly elastic energy, then the relation $(dW/dV)_c = S_c/r_c$ applies such that S_c is directly associated with the more common fracture toughness parameter K_{1c}:

$$S_c = \frac{(1+\nu)(1-2\nu)K_{1c}^2}{2\pi E} \qquad (5)$$

where ν is the Poisson's ratio and K_{1c} the valid ASTM toughness parameter [3] that refers to the sudden release of energy by a macrocrack regardless of whether irreversible deformation has occurred prior to fracture or not. It would therefore be less confusing to consider S_c or K_{1c} as *material behavior* parameters rather than material constants.

CHAPTER 3: FINITE ELEMENT FORMULATION

3.1 General Remarks

When the geometry of the solid under consideration becomes complicated, it is necessary to resort to numerical method. The advent of finite element method has enabled the analysts to resolve many problems that are not amendable to closed form solutions. The procedure involves discretizing a continuum by a finite number of elements in triangular or quadrilateral shape. Variational principles are then applied to minimize certain functions such that the appropriate displacement and/or stress field can be obtained. Such a discretization process invokes certain approximation on the solution of the differential equations that govern stresses, displacements, temperature, etc. The selection of grid pattern and size depends mostly on experience and a prior knowledge of the behavior of local solution, if possible. A normal procedure for developing the appropriate finite element mesh is to check the results with a sample problem whose solution is already known. This, however, does not guarantee accuracy when the geometry and boundary condition are altered. The governing equations can be derived from the principle of Minimum Potential Energy while the finite element formulations from the variational principles [8]. This leads to a system of linear algebraic equations of the form:

$$\sum_{i=1}^{m} K_{ij} u_i = R_j \qquad (6)$$

where u_i are nodal values of the field variables, K_{ij} are the component of the global stiffness matrix, R_j is the global load vector and m is the total number of degrees of freedom of the system.

3.2 Displacement Expression

In two dimensions, the displacement field at a point (x,y) consists of two components:

$$u_x = \sum_{i=1}^{m} [N_i(s,t)(u_x)_i]_e$$

$$u_y = \sum_{i=1}^{m} [N_i(s,t)(u_y)_i]_e \qquad (7)$$

The interpolation function $N_i(s,t)$ relates the point (s,t) in the mapped plane to those in the physical plane (x,y), Figure 3. This provides the relations for (x,y) in terms of the nodal points coordinate (x_i,y_i)

$$x = \sum_{i=1}^{m} [N_i(s,t)x_i]_e$$

$$y = \sum_{i=1}^{m} [N_i(s,t)y_i]_e \qquad (8)$$

It follows from the strain-displacement relations that the strain components ε_x, ε_y and γ_{xy} can also be discretized as:

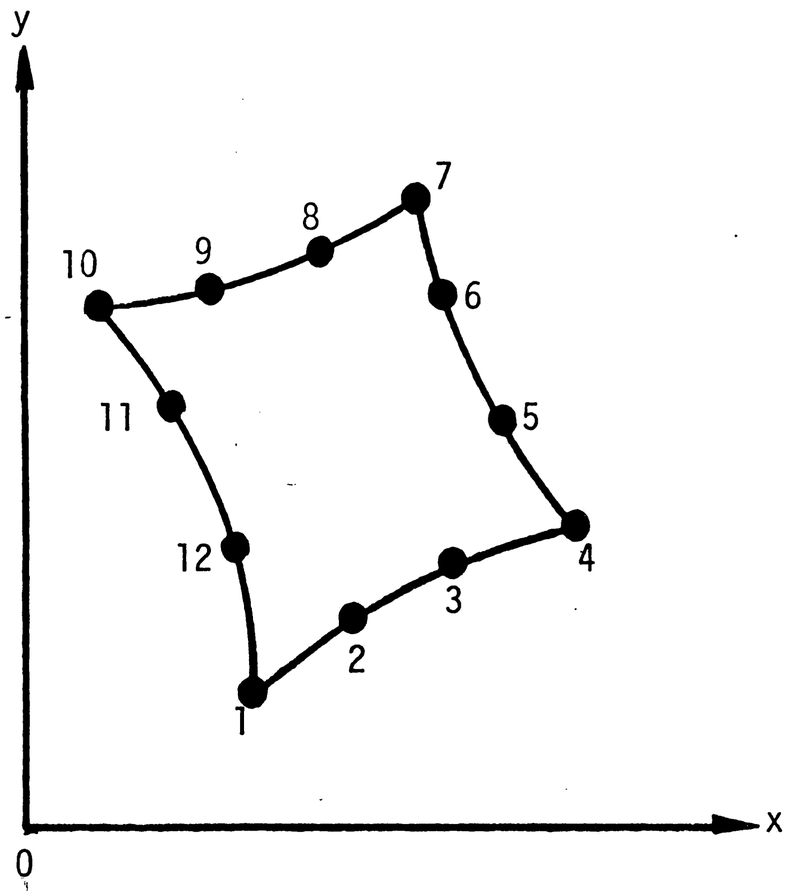

(a) Physical plane

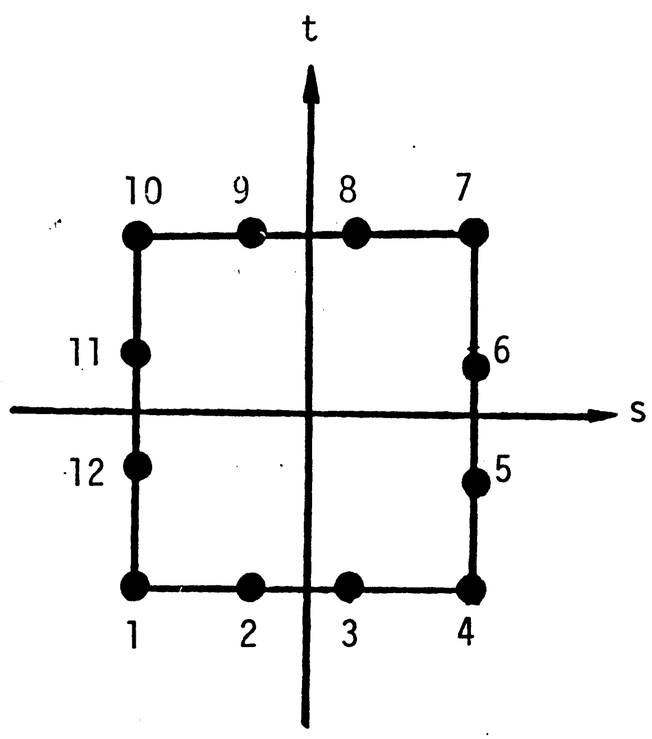

(b) Mapped plane

Figure 3 - Coordinate mapping for 12-nodes isoparametric element.

$$\varepsilon_x = \sum_{i=1}^{m} \left[\frac{\partial(N)_i}{\partial(x)} (u_x)_i\right]_e$$

$$\varepsilon_y = \sum_{i=1}^{m} \left[\frac{\partial(N)_i}{\partial(y)} (u_y)_i\right]_e \tag{9}$$

$$\gamma_{xy} = \sum_{i=1}^{m} \left[\frac{\partial(N)_i}{\partial(y)} (u_x)_i + \frac{\partial(N)_i}{\partial(x)} (u_y)_i\right]_e$$

3.3 Uncoupled Linear Isotropic Thermal Elasticity [9]

The formulation assumes that the temperature field can be determined independently of the deformations of the body. The material behaves elastically at all times and undergoes small deformation.

The relations between stress and strain are given by

$$\varepsilon_{ij} = \frac{1+\nu}{E} \sigma_{ij} - \frac{\nu}{E} \sigma_{kk}\delta_{ij} + \alpha(T-T_o)\delta_{ij}$$

$$\sigma_{ij} = 2G\left[\varepsilon_{ij} + \frac{\nu}{1-2\nu} \sigma_{kk}\delta_{ij} - \frac{1+\nu}{1-2\nu} \alpha(T-T_o)\delta_{ij}\right] \tag{10}$$

In particular, dW/dV is dependent not only on the state of stress and strain but the level of thermal energy. Let the temperature at a given point in the solid be $T(x,y,z)$ and T_o be a constant reference temperature. The expression for dW/dV in linear thermal elasticity is

$$\frac{dW}{dV} = \frac{1}{2E}\left[(1+\nu)\sigma_{ij}\sigma_{ij} - 2\sigma_{kk}^2\right] = G\left[\varepsilon_{ij}\varepsilon_{ij} + \frac{\nu}{1-2\nu}\varepsilon_{kk}^2\right.$$

$$\left. - \frac{2(1+\nu)}{1-2\nu}\alpha(T-T_o)\varepsilon_{kk}\right] + 3G\frac{1+\nu}{1-2\nu}\alpha^2(T-T_o)^2 \qquad (11)$$

where G is the shear modulus, α is the coefficient of thermal expansion and σ_{kk} is the first stress invariant.

3.4 Finite Element Analysis

The analysis consists of the determination of temperature and stress distribution.

3.4.1 Heat Conduction

The heat conduction portion of the problem is solved by using a finite element code written by Robert Bolton [10]. The finite element equations are derived from the variational principle. Linear shape function are used with triangular element. The steady-state temperature distribution is then used as the input to a separate stress analysis computer program.

3.4.2 Stress Distribution

Stress analysis is performed using a two dimensional and axisymmetric program (APES) [11] developed by Naval Ship Research and Development Center jointly with Lehigh University. It employs the twelve-node isoparametric elements with consideration given to solution accuracy in terms of the relative sizes of the element. This re-

sults in a cubic variation of the displacement field. Curvilinear elements in the physical plane are transformed to cubes in the mapped plane by application of the shape functions. A total of twelve nodes on each element are used in the isoparametric sense. Integration is carried out by using the Gauss-Legendre quadrature technique in the mapped plane. The three or four point approximation is available in the APES program. A frontal solution technique is chosen for solving the system of linear algebraic equations. Accuracy of the local solution is achieved by placing four side nodes at 1/9 and 4/9 distance from the corner node at the crack tip. The 1/r singularity of the strain energy density function is thus preserved at these boundaries. Although the numerical values of dW/dV at the nodes may vary depending on the interpolation scheme, this uncertainty is overcome by interpreting the values of dW/dV at the quadrature points of each element in the form of contour plots.

CHAPTER 4: TEMPERATURE FIELD AND CRACK GROWTH

In order to establish the crack-resistance curve under thermal-loading, sudden temperature change is imposed while the stress state is assumed to be quasi-static in nature. Six temperature increments are taken with an initial reference temperature T_o for two different kinds of boundary conditions.

4.1 Material Properties

The material selected for the cracked specimen is a typical engineering steel alloy with the following properties:

$$\nu = 0.33$$

$$E = 206.84 \times 10^3 \text{ MPa } [30 \times 10^3 \text{ ksi}]$$

$$\sigma_{yd} = 5.1711 \times 10^2 \text{ MPa } [7.5 \times 10^4 \text{ psi}]$$

$$\alpha = 6 \times 10^{-5} \text{ m/m/°C} \qquad (12)$$

$$K_{Ic} = 82.416 \text{ MPa}\cdot\text{m } [75 \times 10^3 \text{ psi}\sqrt{\text{in}}]$$

$$S_c = 3.275 \times 10^3 \text{ N/m } [18.7 \text{ lb}_f/\text{in}]$$

$$\left(\frac{dW}{dV}\right)_c = \frac{\sigma_{yd}^2}{2E} = 646.406 \text{ KPa } [93.75 \text{ psi}]$$

Thermal loading is applied incrementally as the crack grows in accordance with equation (2). The yield strength σ_{yd} should, in general, be adjusted for different thermal state. In the present work,

the variations of the temperature range is not large enough to warrant such a change. Hence, the same $(dW/dV)_c$ value will be used to determine the failure of elements ahead of the crack.

4.2 Geometric Configuration and Boundary Conditions

A centrally cracked panel under the condition of plane strain is considered. Because of symmetry, only one quarter of the problem needs to be analyzed. Refer to Figure 4 for the dimensions of the panel with a central crack of length 5.08 cm. The finite element grid patterns used in heat conduction and stress analysis are shown in Figures 5 and 6, respectively.

Two types of boundary conditions will be treated. The first assumes that the crack surface temperature is raised from T_o to T_1 while the panel outer edges are kept at uniform temperature. This condition can be specified as

$$T(x,y) = T_o - T_o = 0 \text{ for } y = \pm 25.40 \text{ cm}$$

$$\frac{\partial T}{\partial x} = 0 \text{ for } x = \pm 12.70 \text{ cm} \qquad (13)$$

$$T(x,y) = T_1 - T_o \text{ for } y = \pm 0,\ -a<x<a$$

The second boundary value problem is concerned with a partially insulated crack that grows incrementally while the temperature at the crack edge is raised in steps of ΔT, i.e.,

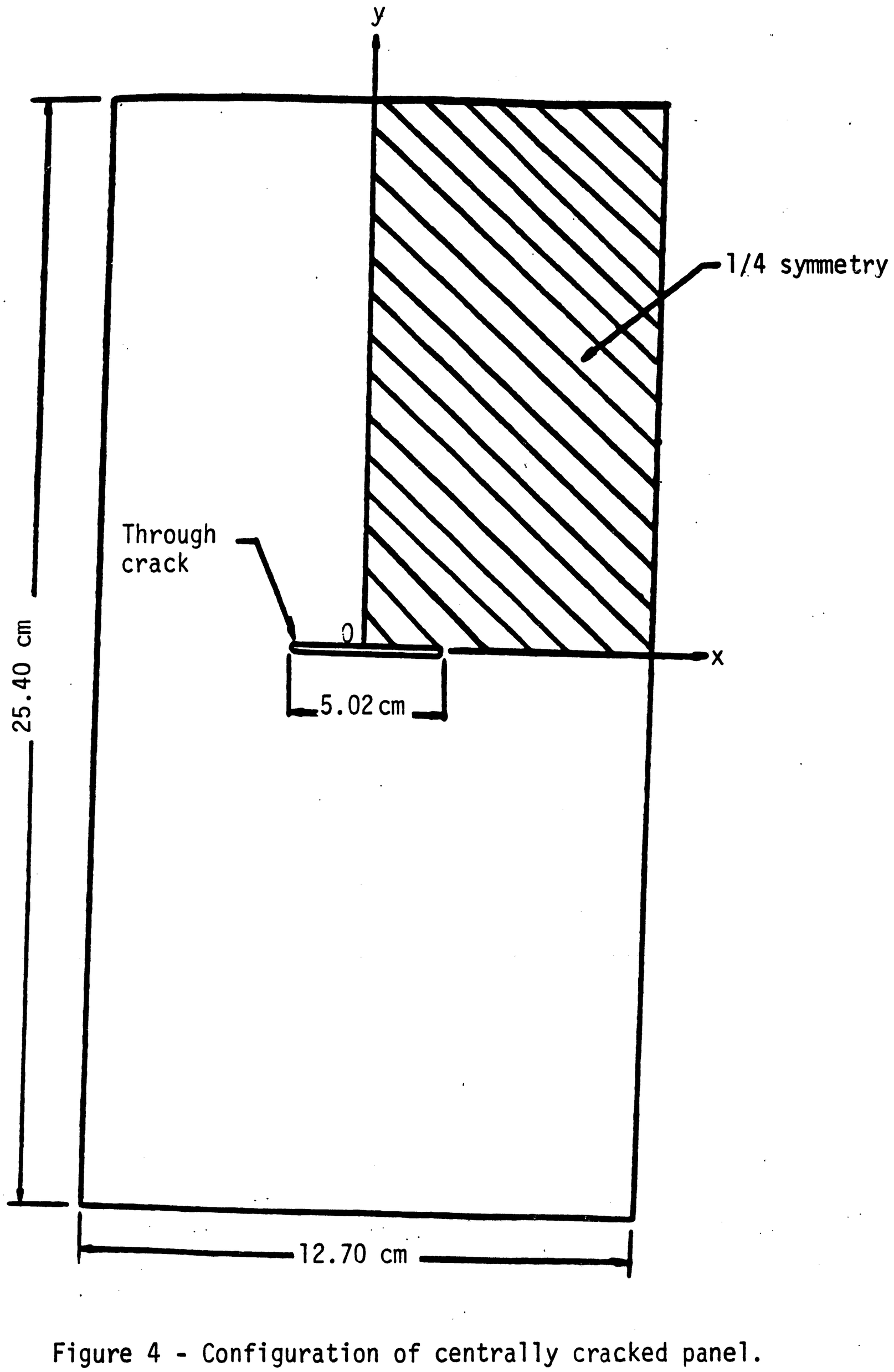

Figure 4 - Configuration of centrally cracked panel.

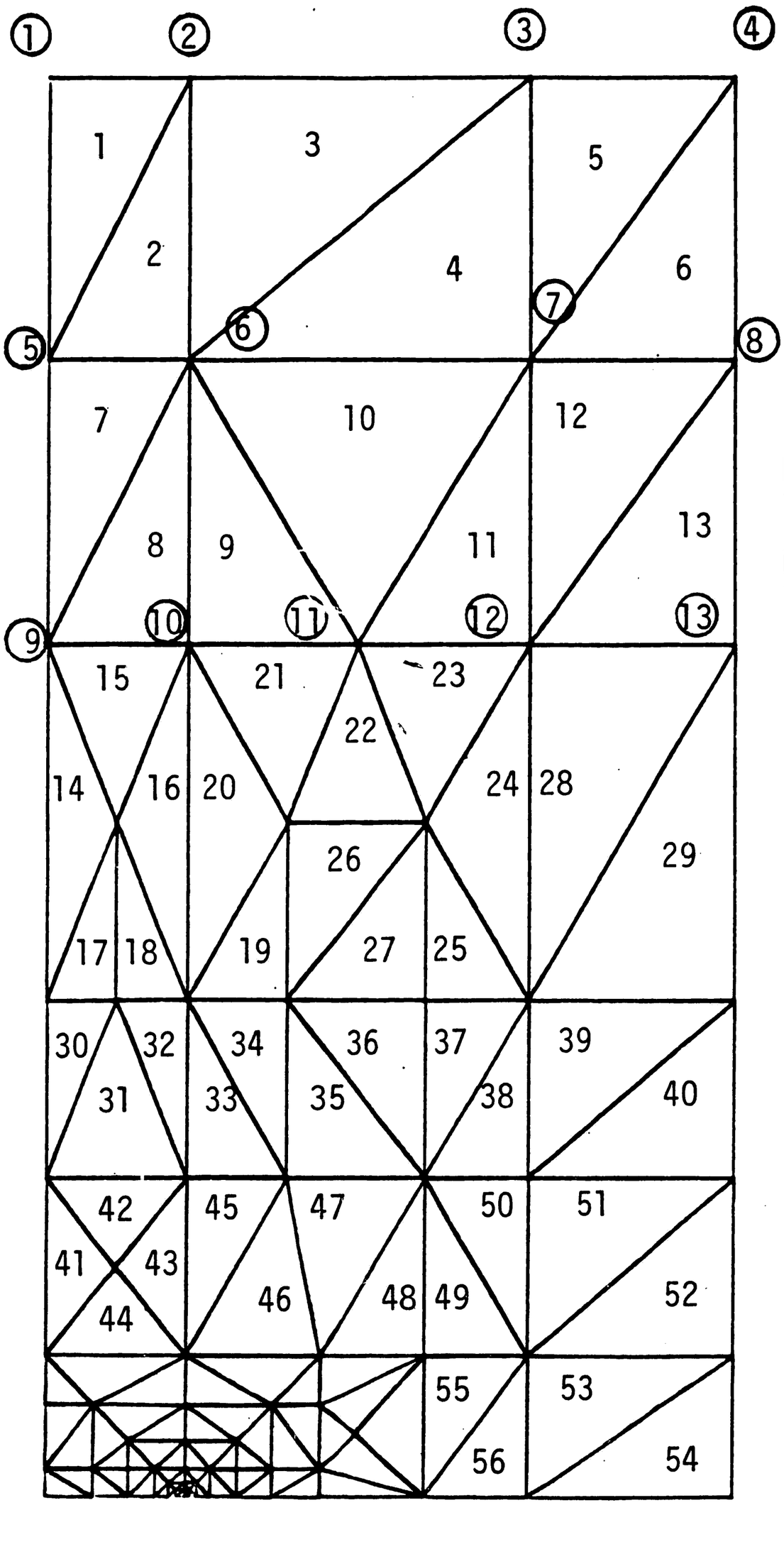

No. of elements:
118

No. of nodes:
76

Figure 5 - Triangular finite element grid pattern used in heat conduction.

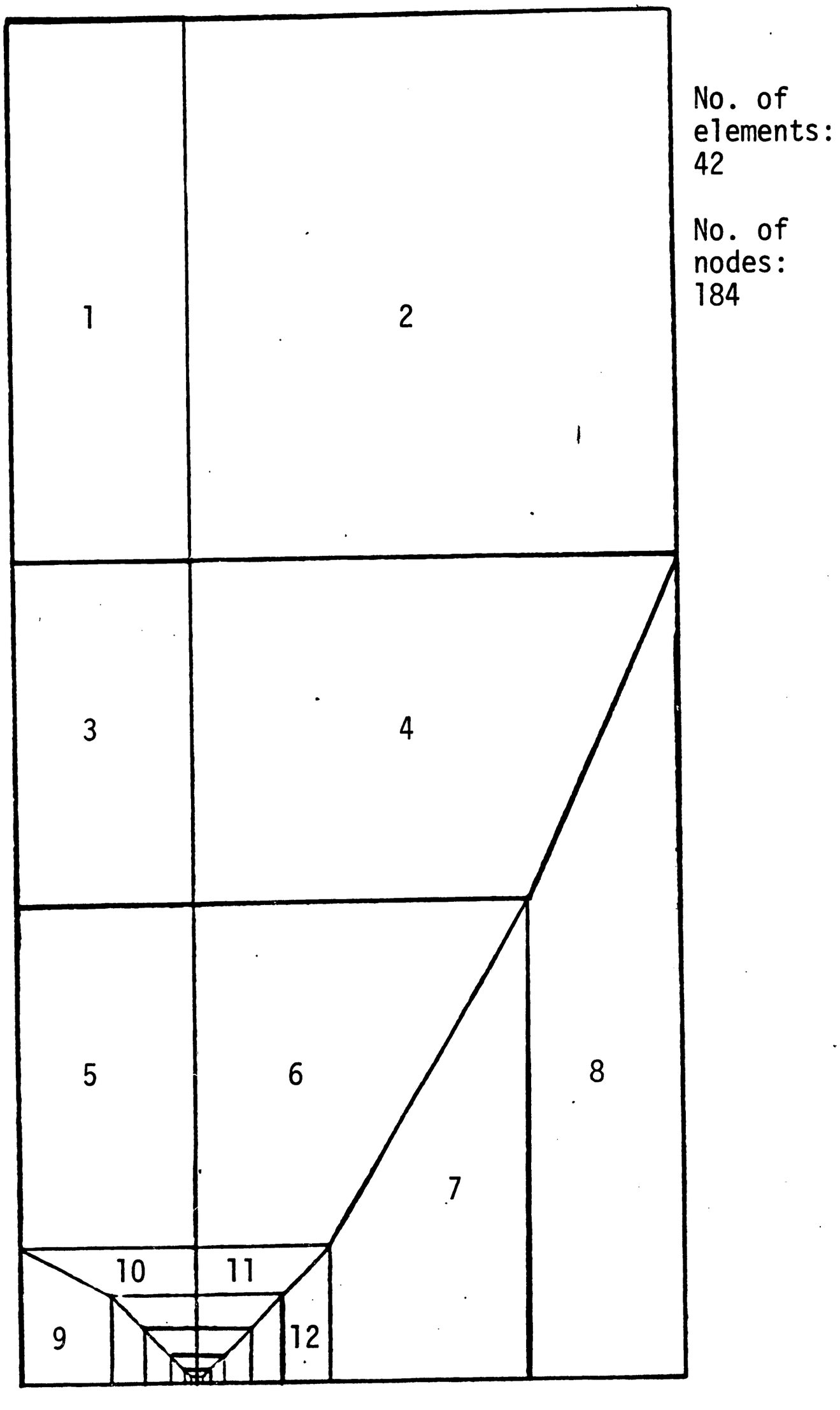

Figure 6 - Finite element grid pattern used in stress analysis.

$$T(x,y) = T_1 - T_o \text{ for } y = \pm 25.40 \text{ cm}$$

$$\frac{\partial T}{\partial x} = 0 \text{ for } x = \pm 12.70 \text{ cm} \qquad (14)$$

$$\frac{\partial T}{\partial y} = 0.5 \left(\frac{\partial T}{\partial y}\right)_o \text{ for } y = \pm 0 \quad -a<x<a$$

In equation (14), $(\partial T/\partial y)_o$ denotes the undisturbed temperature gradient or q/K, i.e., the normalized heat transfer. This is equivalent to specifying 50% of heat loss in a partially insulated crack surface. Here, q is the heat flux and is assumed to correspond to the case of 50% heat loss with K being the heat conductivity.

4.3 Temperature Rise on Crack Surface

Using the grid pattern in Figure 5, the temperature distribution in a cracked panel is first determined according to the boundary condition in equation (13). The temperature on the crack is increased in steps starting from an initial crack of length 2a = 5.08 cm or a = 2.54 cm. A total of six steps are taken as indicated in Table 1. Figure 7 displays the constant temperature profiles in one-quarter of the panel when the crack has grown to a length of 2a = 7.748 cm. The gradual diffusion of temperature intensity with distance from the crack is noticeable. Note that the crack no longer has any influence on the temperature when $\Delta T \simeq 27°C$, Figure 7.

Plotted in Figures 8 to 13 inclusive are the strain energy density function versus radial distance ahead of the crack. Correspond-

Table 1 - Crack growth data for temperature specified on crack surface.

Crack Growth Step Number	Temperature Increment $(T-T_o)(°C)$	Half Crack Length a (cm) (in)	S.E.D. Factor S 10^3 (N/m) (lb_f/in)
1	28.54	2.588 1.019	0.312 1.7813
2	38.56	2.692 1.060	0.673 3.8438
3	48.54	2.832 1.115	0.903 5.1563
4	58.54	3.067 1.207	1.520 8.6813
5	68.54	3.414 1.344	2.240 12.7875
6	78.54	3.874 1.525	2.970 16.9690

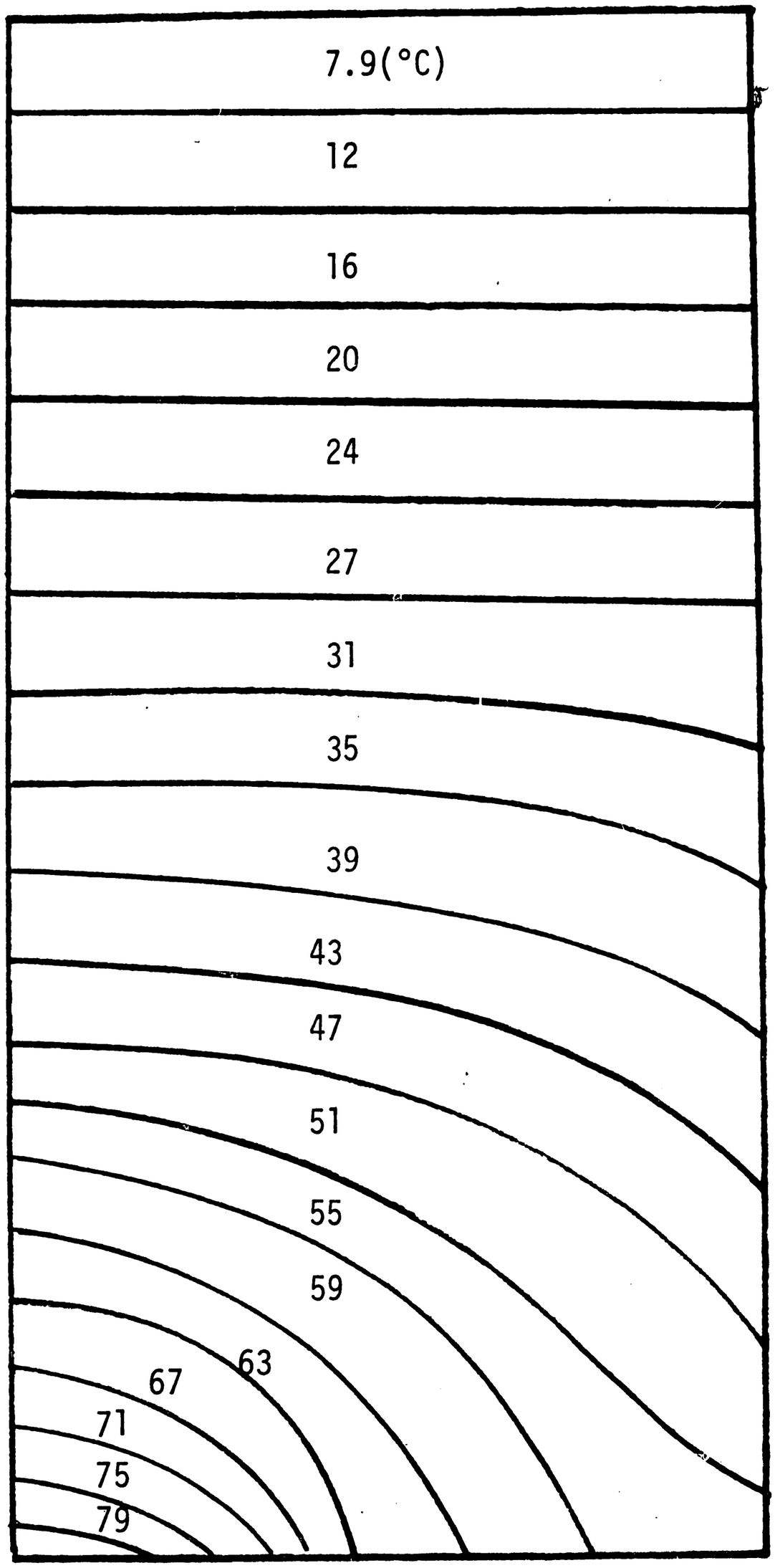

Figure 7 - Constant temperature contours for crack with surface temperature rise - crack growth step no. 6.

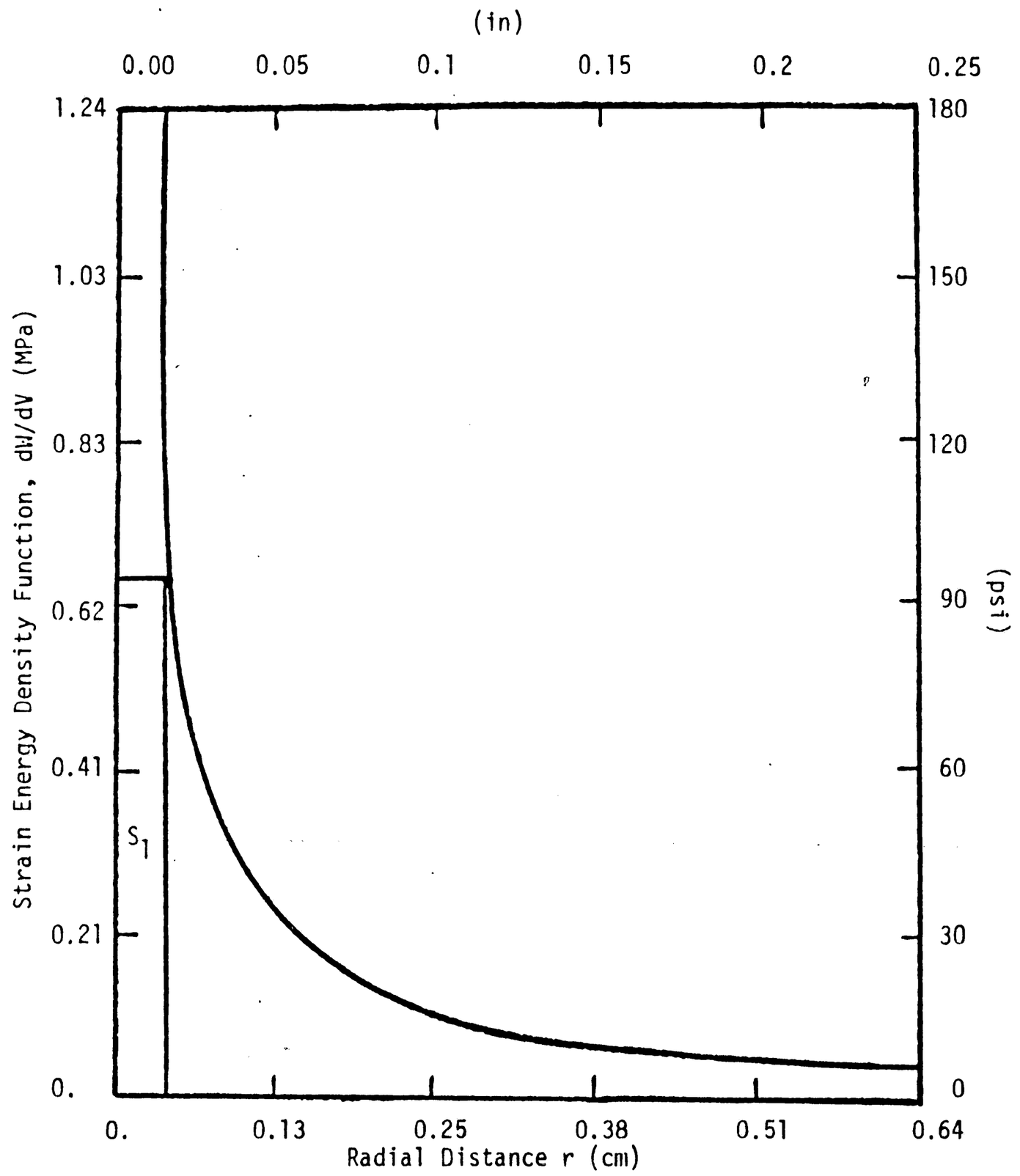

Figure 8 - Variation of dW/dV versus distance for crack growth, step no. 1 with equation (13) as boundary condition.

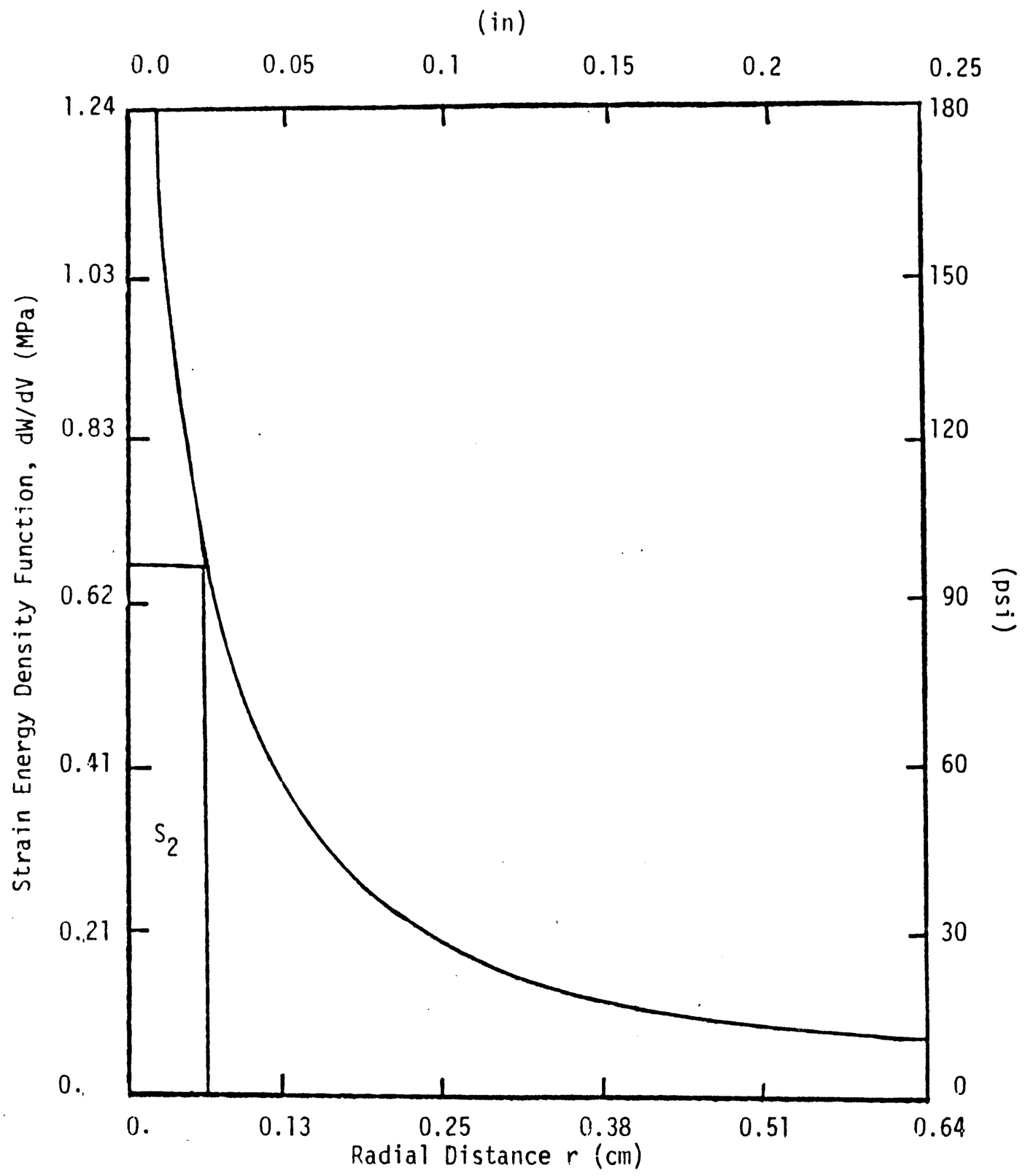

Figure 9 - Variation of dW/dV versus distance for crack growth, step No. 2 with equation (13) as boundary condition.

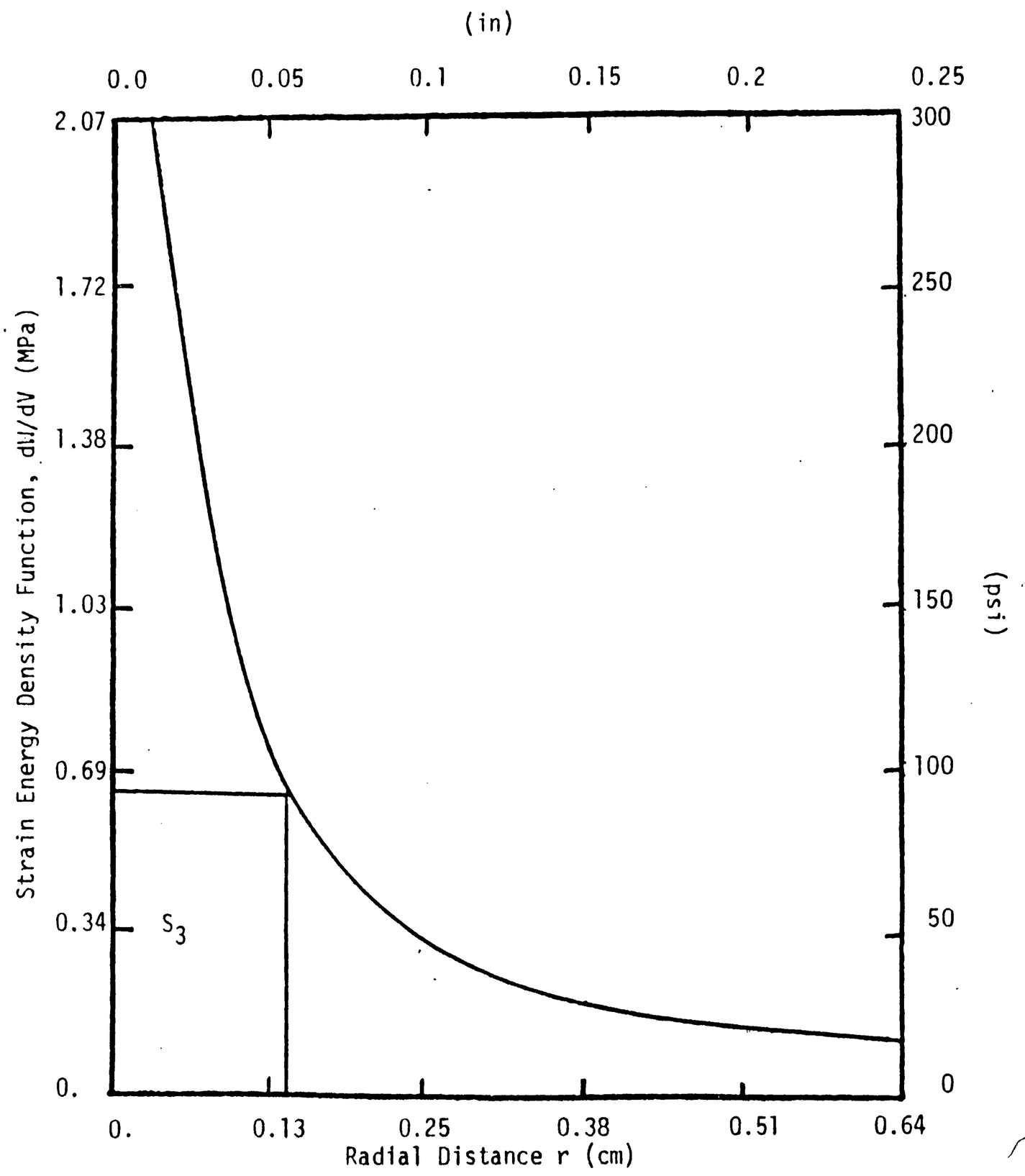

Figure 10 - Variation of dW/dV versus distance for crack growth, step no. 3 with equation (13) as boundary condition.

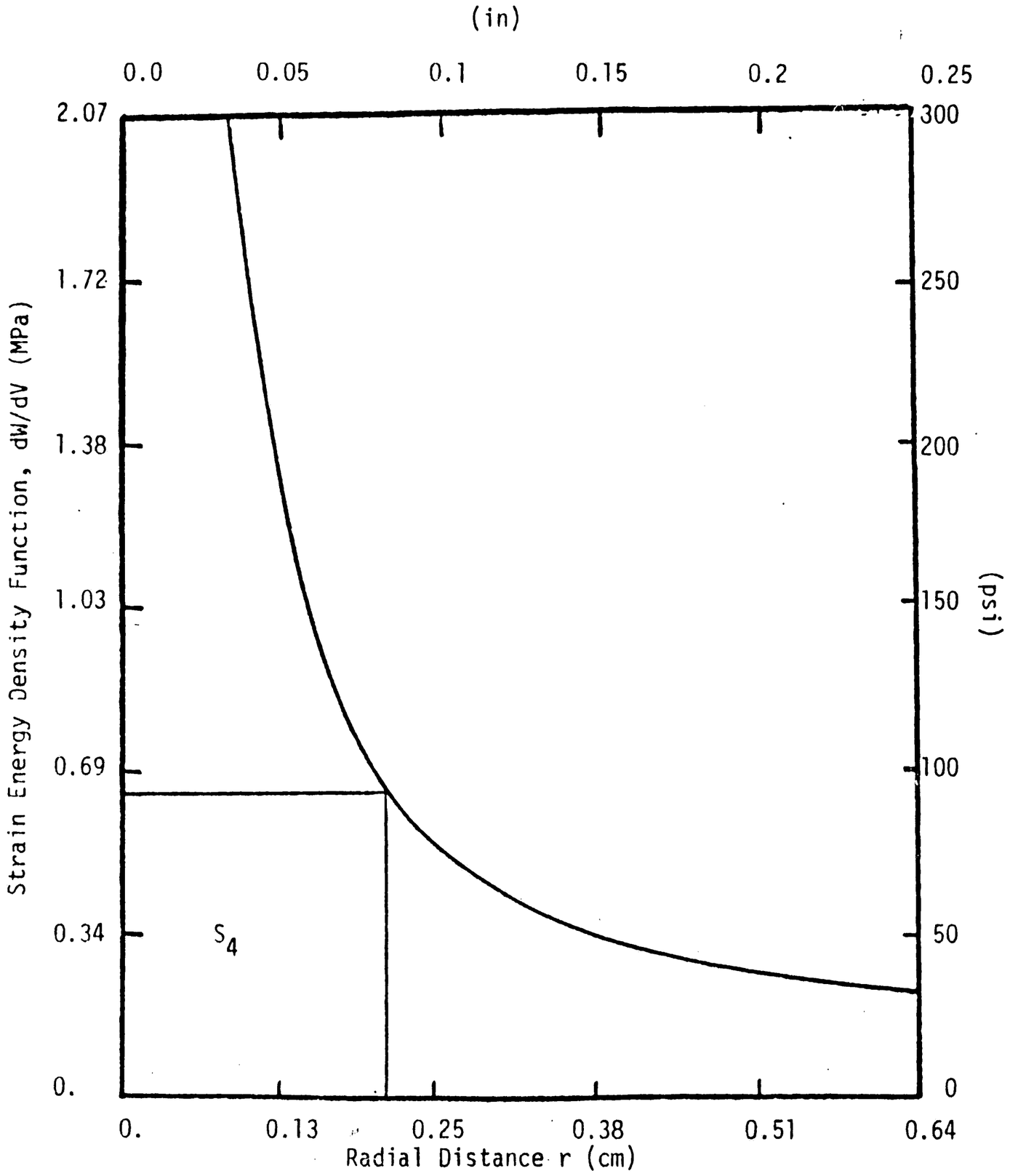

Figure 11 - Variation of dW/dV versus distance for crack growth, step no. 4 with equation (13) as boundary condition.

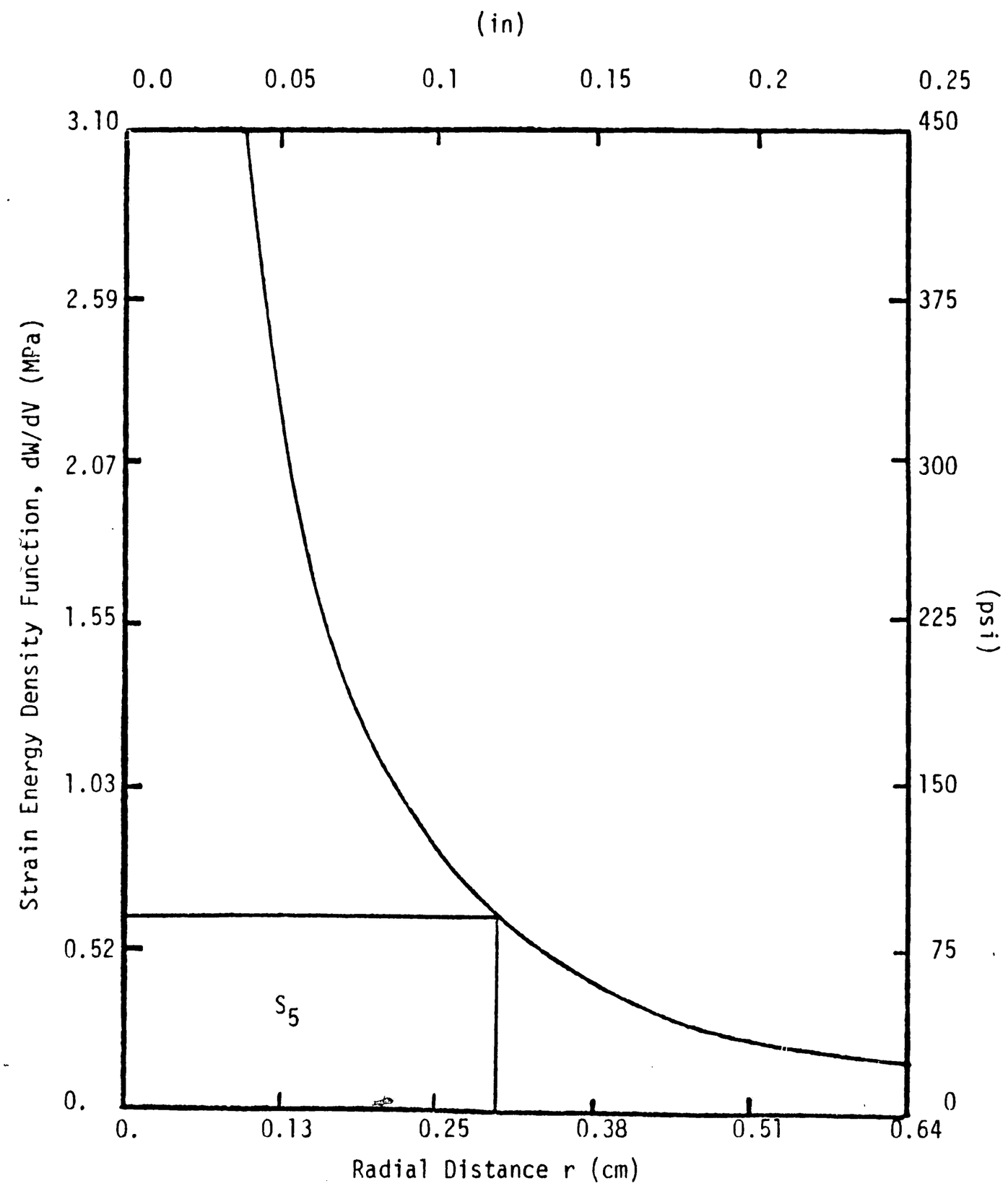

Figure 12 - Variation of dW/dV versus distance for crack growth, step no. 5 with equation (13) as boundary condition.

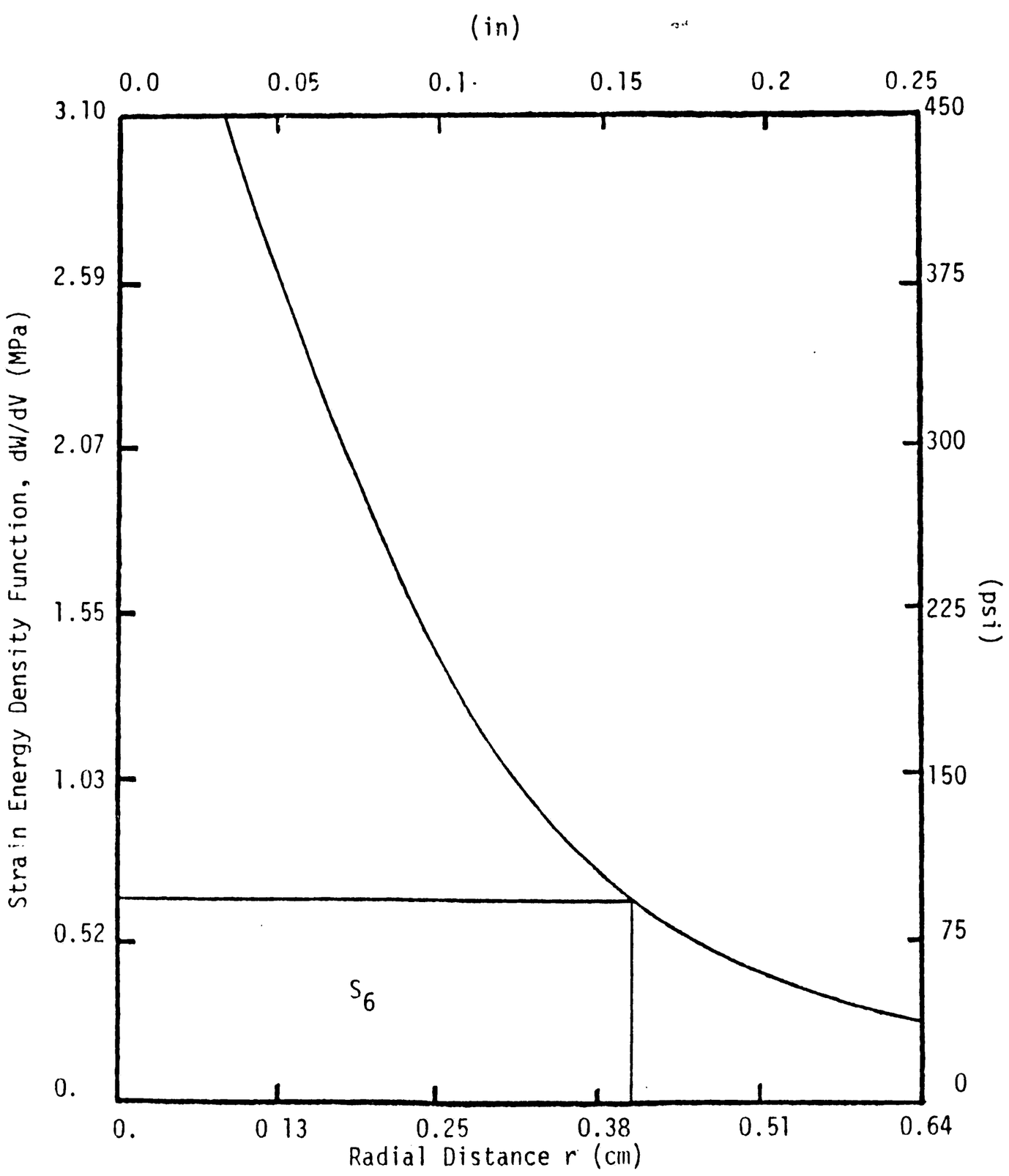

Figure 13 - Variation of dW/dV versus distance for crack growth, step no. 6 with equation (13) as boundary condition.

ing to the six growth steps in Table 1. All results are calculated by taking a core region of r_o = 0.056 cm. In general, all the curves rise very high near the crack tip and their magnitude always quickly with the distance r. Each segment of growth r_1, r_2, etc., is determined from the intersection of the curve with the critical value of $(dW/dV)_c$ = 646.41 KPa as given in equation (13). The areas S_1, S_2, etc., increased in accordance with the inequalities of equation (3). This indicates that the crack growth process is unstable. Table 1 gives the successive values of crack growth and the corresponding strain energy density factor. At the sixth step, S = 2.970×10^3 N/m which is nearly equal to S_c = 3.275×10^3 N/m at which point the crack propagates rapidly.

4.4 Partially Insulated Crack

The temperature on the panel edges at y = ±25.40 cm are initially kept at ambient temperature T_o. It is then increased in steps of ΔT as shown in Table 2 with a total of six steps. Illustrated in Figure 14 is the constant temperature contours corresponding to the fourth step of crack growth. Again, the influence of the crack disappears as distances sufficiently far away.

Figures 15 to 20 display the plots of the strain energy density function variations with the distance ahead of the crack. The sharp drop in dW/dV is again exhibited and the results depend on the degree of crack surface insulation. The areas $S_1, S_2, \ldots, S_6$ again are found

Table 2 - Crack growth data for a partially insulated crack.

Crack Growth Step Number	Temperature Gradient $(\partial T/\partial y)_o$ (°C/cm)	Half Crack Length a (cm) (in)	S.E.D. Factor S 10^3 (N/m) (lb_f/in)
1	7.88	2.586 1.018	0.296 1.69
2	10.24	2.672 1.052	0.559 3.19
3	12.60	2.819 1.110	0.953 5.44
4	14.96	3.012 1.186	1.259 7.13
5	16.54	3.297 1.298	1.839 10.50
6	18.90	3.724 1.466	2.758 15.75

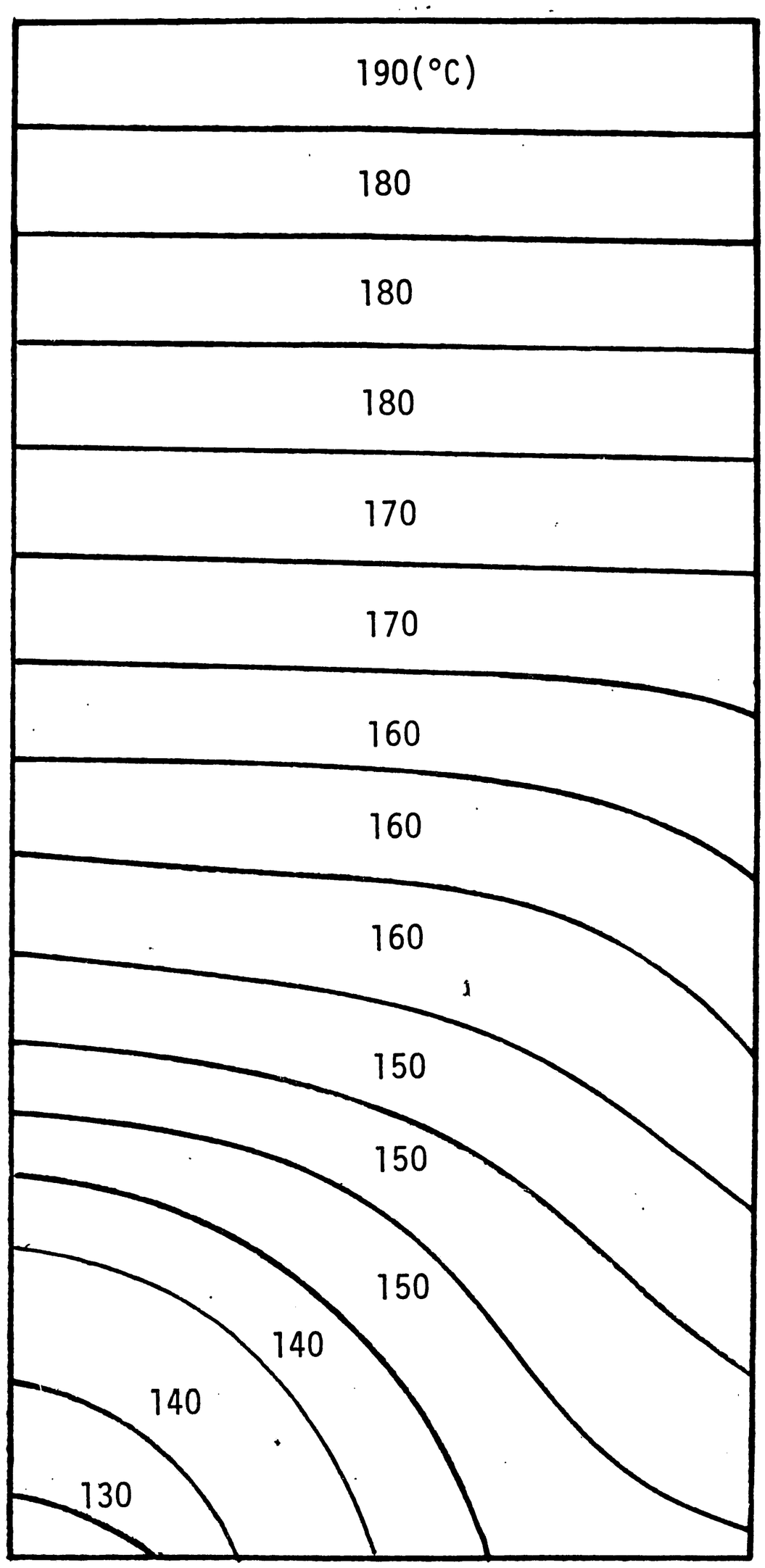

Figure 14 - Contours of constant temperature for a partially insulated crack after four steps of growth.

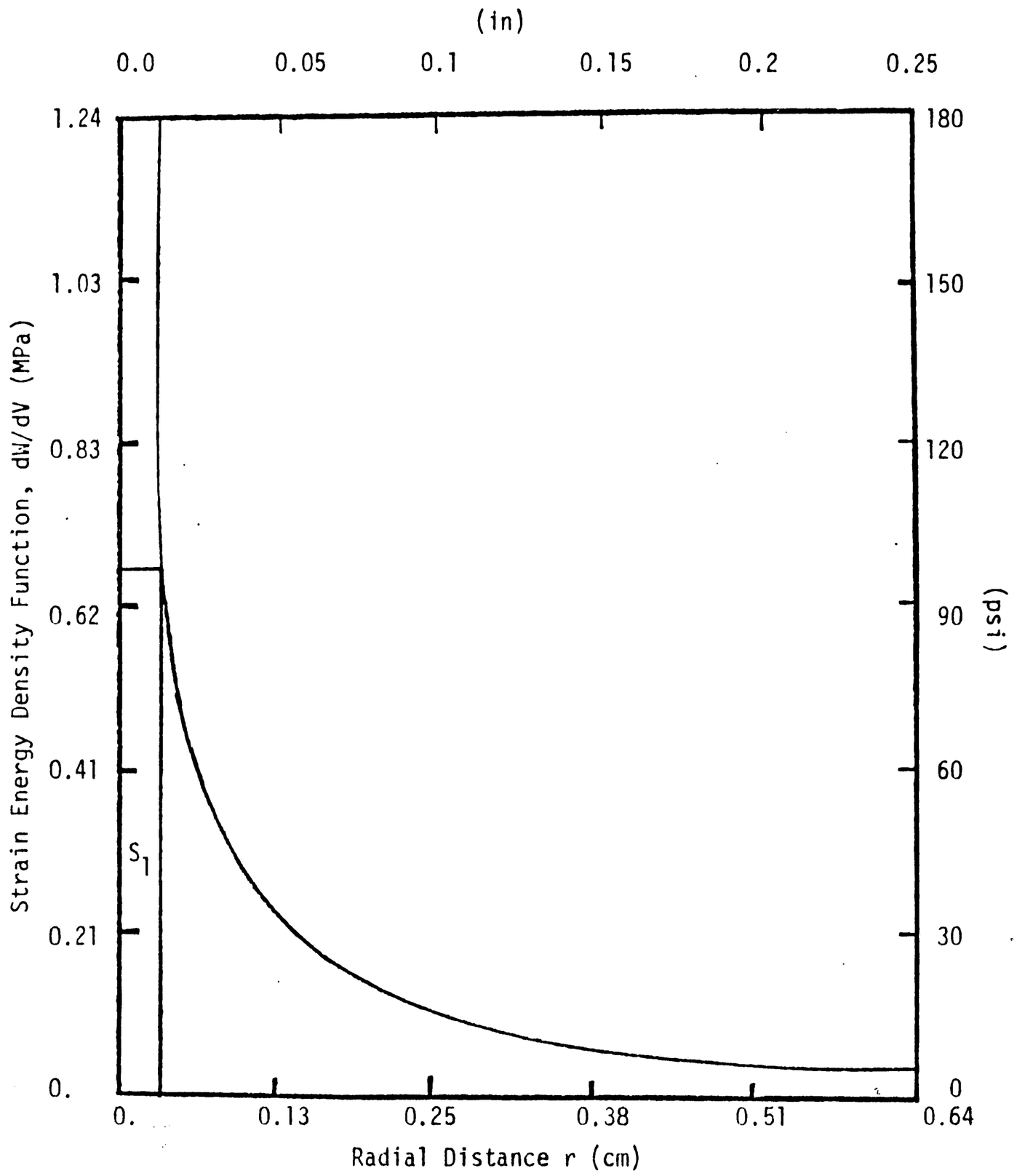

Figure 15 - Variation of dW/dV versus distance for crack growth, step no. 1 with equation (14) as boundary condition.

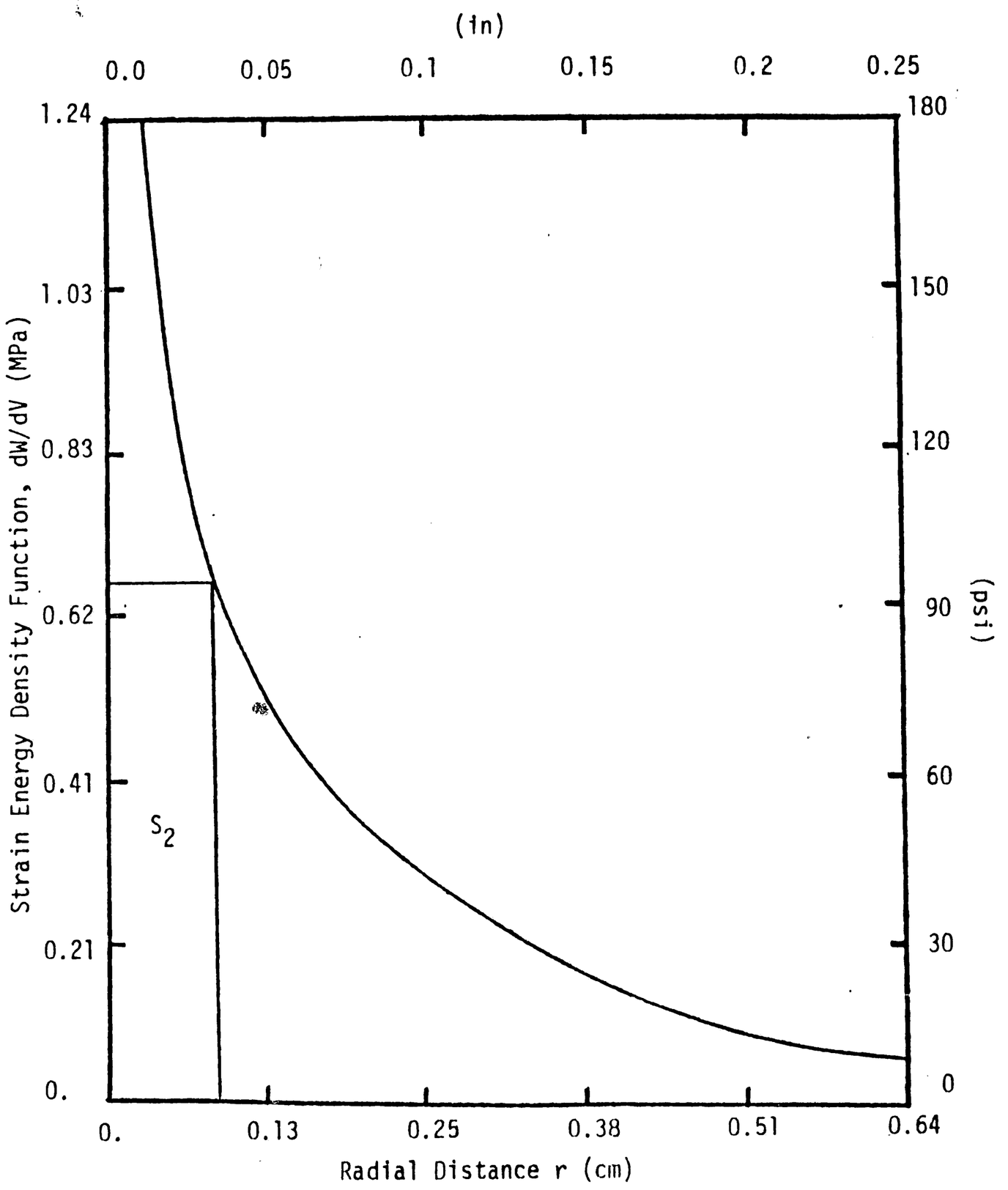

Figure 16 - Variation of dW/dV versus distance for crack growth, step no. 2 with equation (14) as boundary condition.

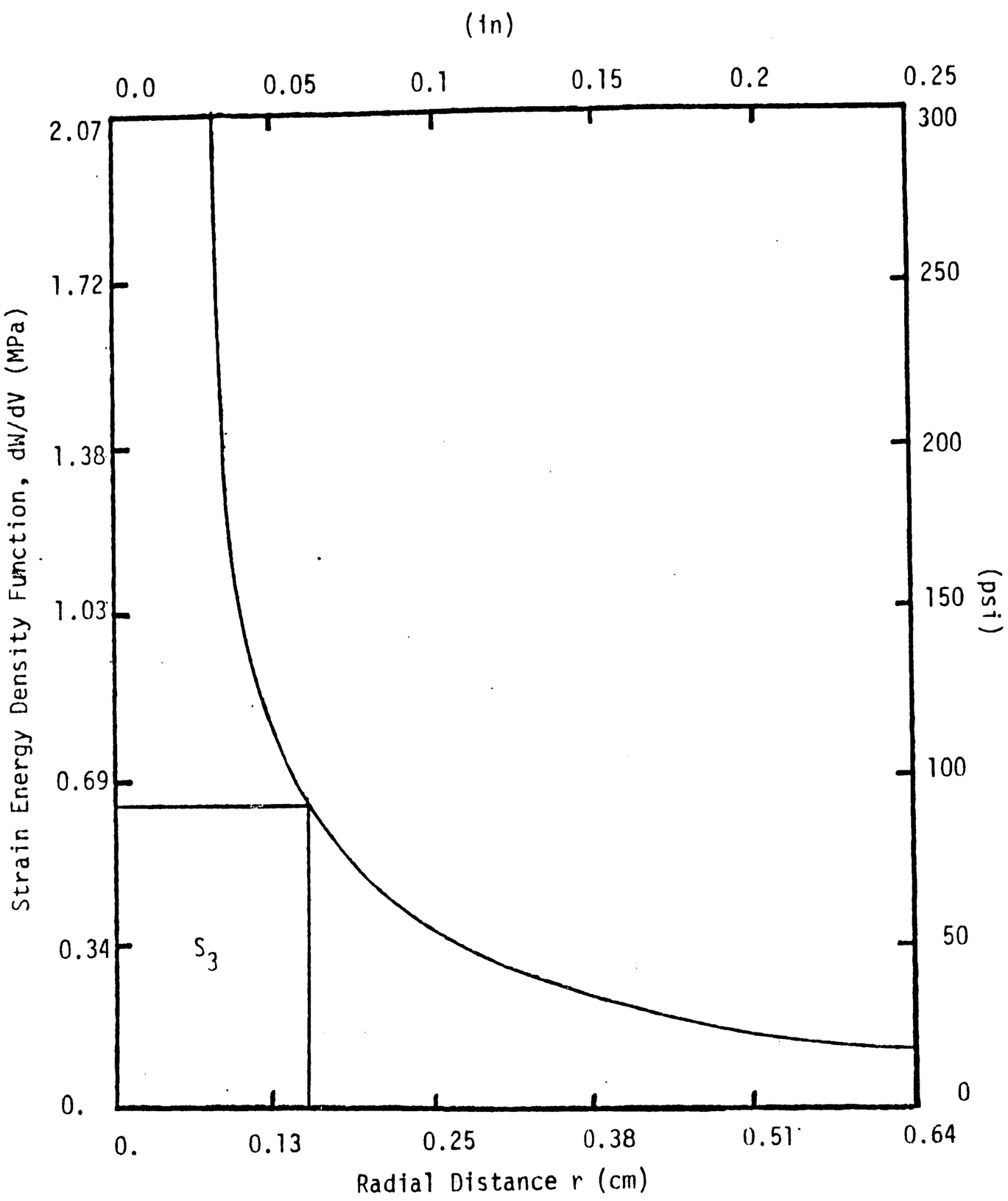

Figure 17 - Variation of dW/dV versus distance for crack growth, step no. 3 with equation (14) as boundary condition.

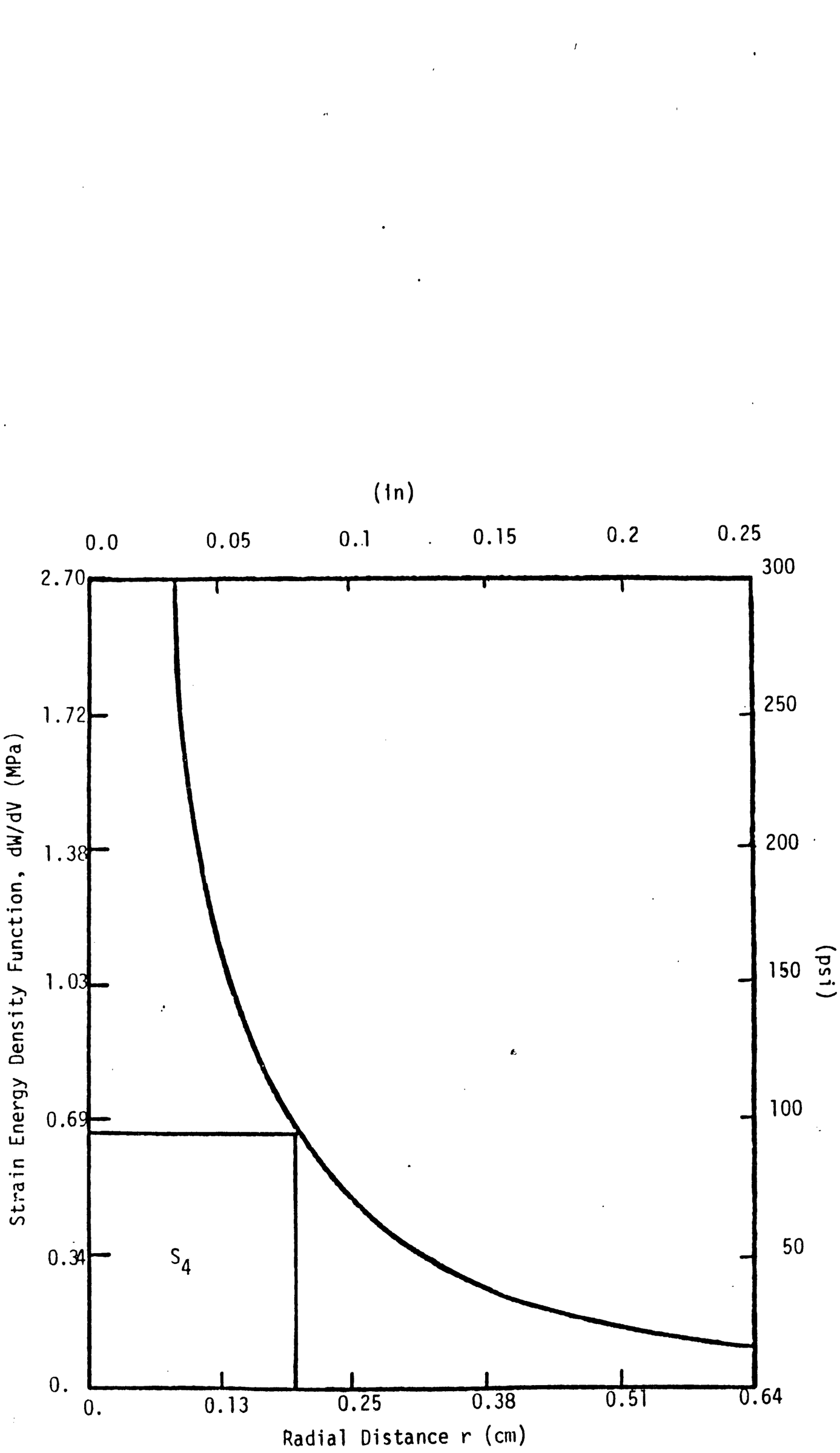

Figure 18 - Variation of dW/dV versus distance for crack growth, step no. 4 with equation (14) as boundary condition.

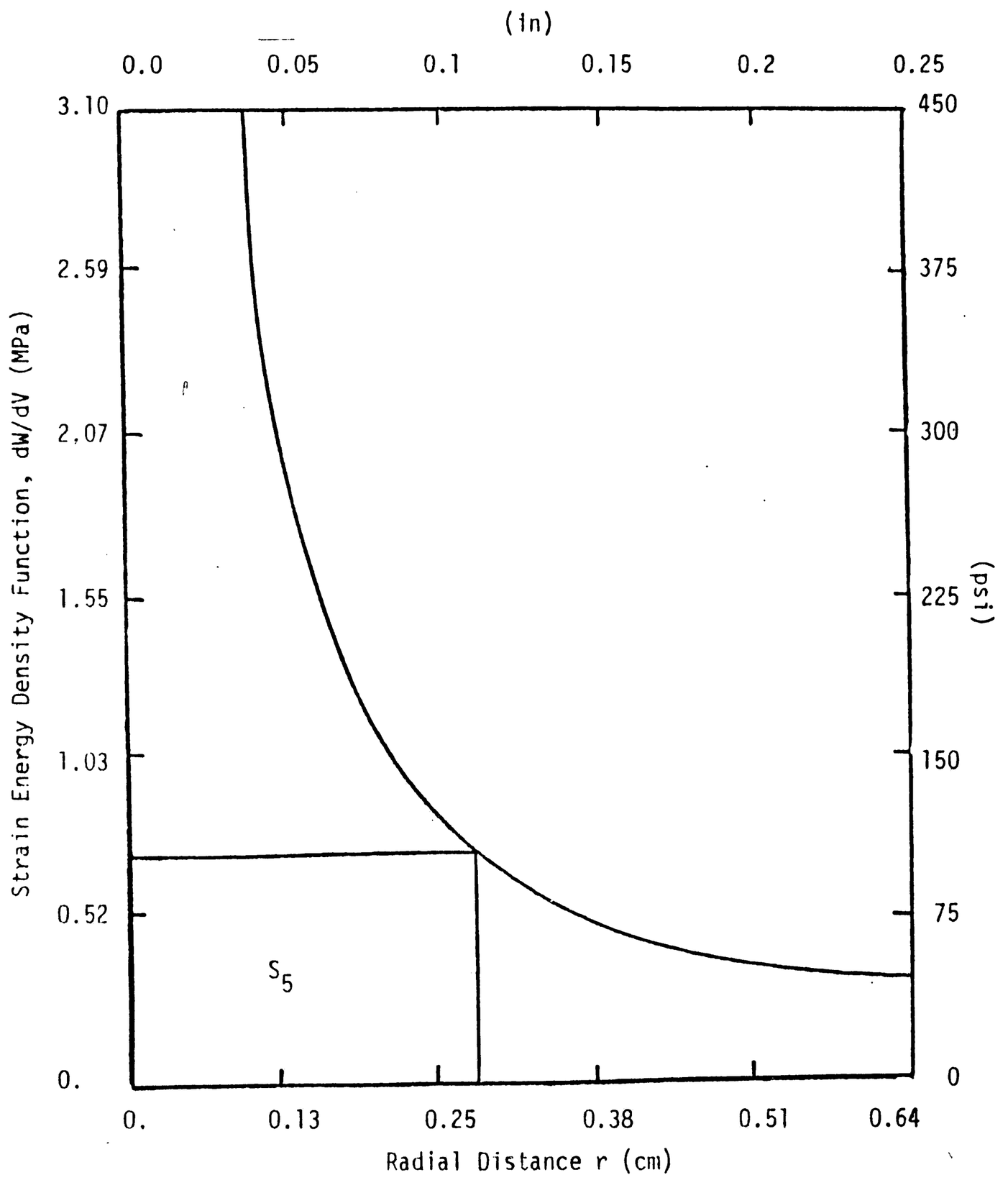

Figure 19 - Variation of dW/dV versus distance for crack growth, step no. 5 with equation (14) as boundary condition.

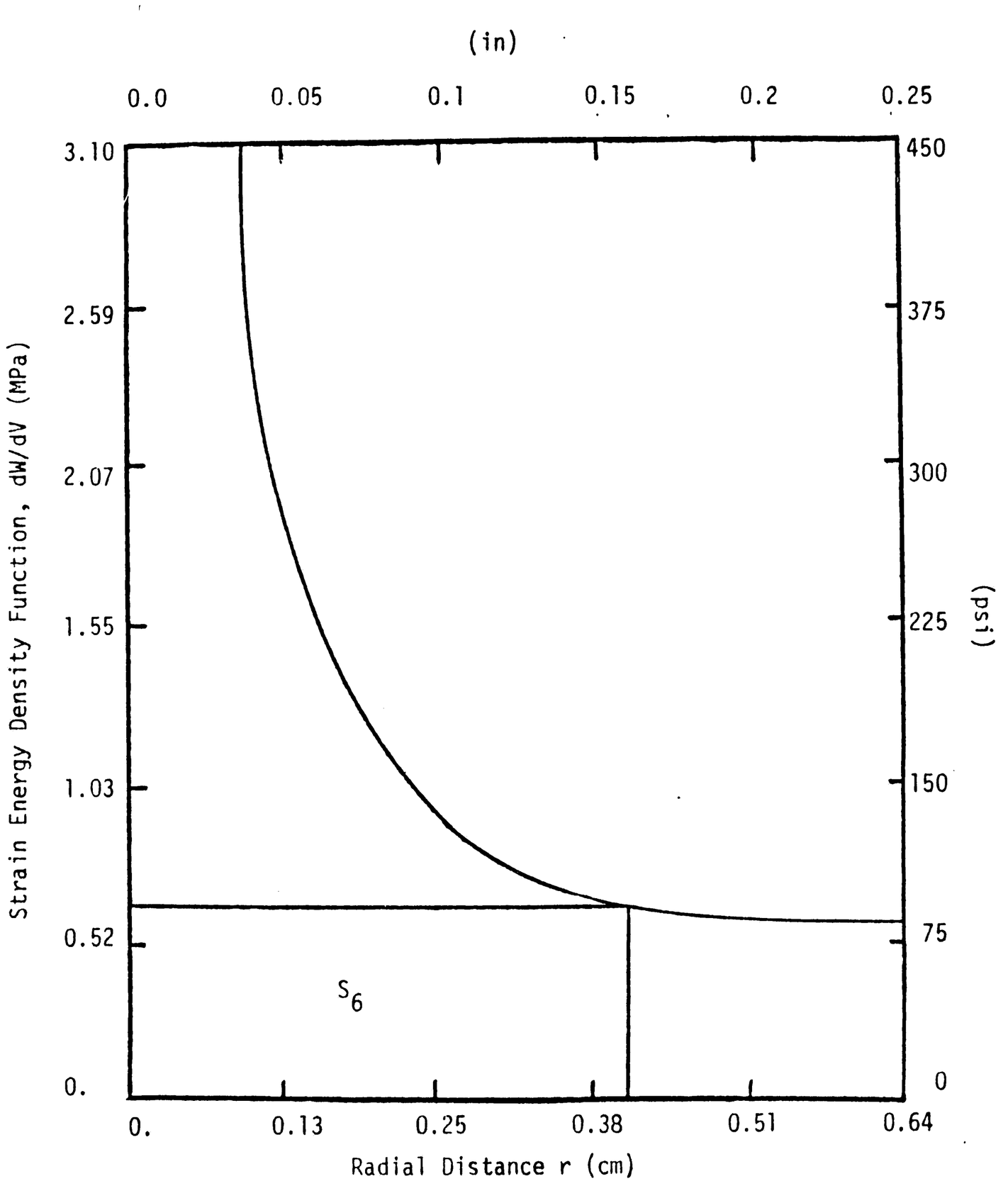

Figure 20 - Variation of dW/dV versus distance for crack growth, step no. 6 with equation (14) as boundary condition.

by establishing the rectangles such that their tops coincide with $(dW/dV)_c$ = 646.41 KPa. The crack growth is also unstable as $r_1 < r_2 < \text{---} < r_6$. This is tabulated in Table 2. The crack leads to stabilize as the insulation on the crack surface is increased. This will be discussed in connection with the crack growth resistance curves.

CHAPTER 5: CRACK GROWTH RESISTANCE CURVES

One of the salient features of the strain energy density criterion is that it linearizes the crack growth data. That is, all results in the strain energy factor versus crack growth plots are straight lines.

Figure 21 gives the results for the strain energy density factor as a function of crack growth. Indeed, a straight line prevails. The advantage of establishing the dS/da = const. relationship is that results to other boundary condition can also be obtained. For instance, the curve in Figure 21 for the case of increasing crack surface temperature may be regarded as that of a crack with no insulation or with perfect heat conduction. In other words, the temperature increments ΔT applied on the panel edges in Table 2 which yield those values shown in Table 1 at the prospective crack sites at each increment of growth. The identical results exhibited in Figure 21 or Table 1 could have been obtained by specifying the third condition in equation (14) as $\partial T/\partial y = (\partial T/\partial y)_o$ on the crack. This is equivalent to the case that all the heat from the surrounding is conducted across the crack surface.

The slope of the dS/da curve in Figure 22 is seen to increase when the crack surface resists heat transfer by fifty percent. Further increase in crack surface insulation will rotate the dS/da = const. line even more in the counterclockwise direction. In the

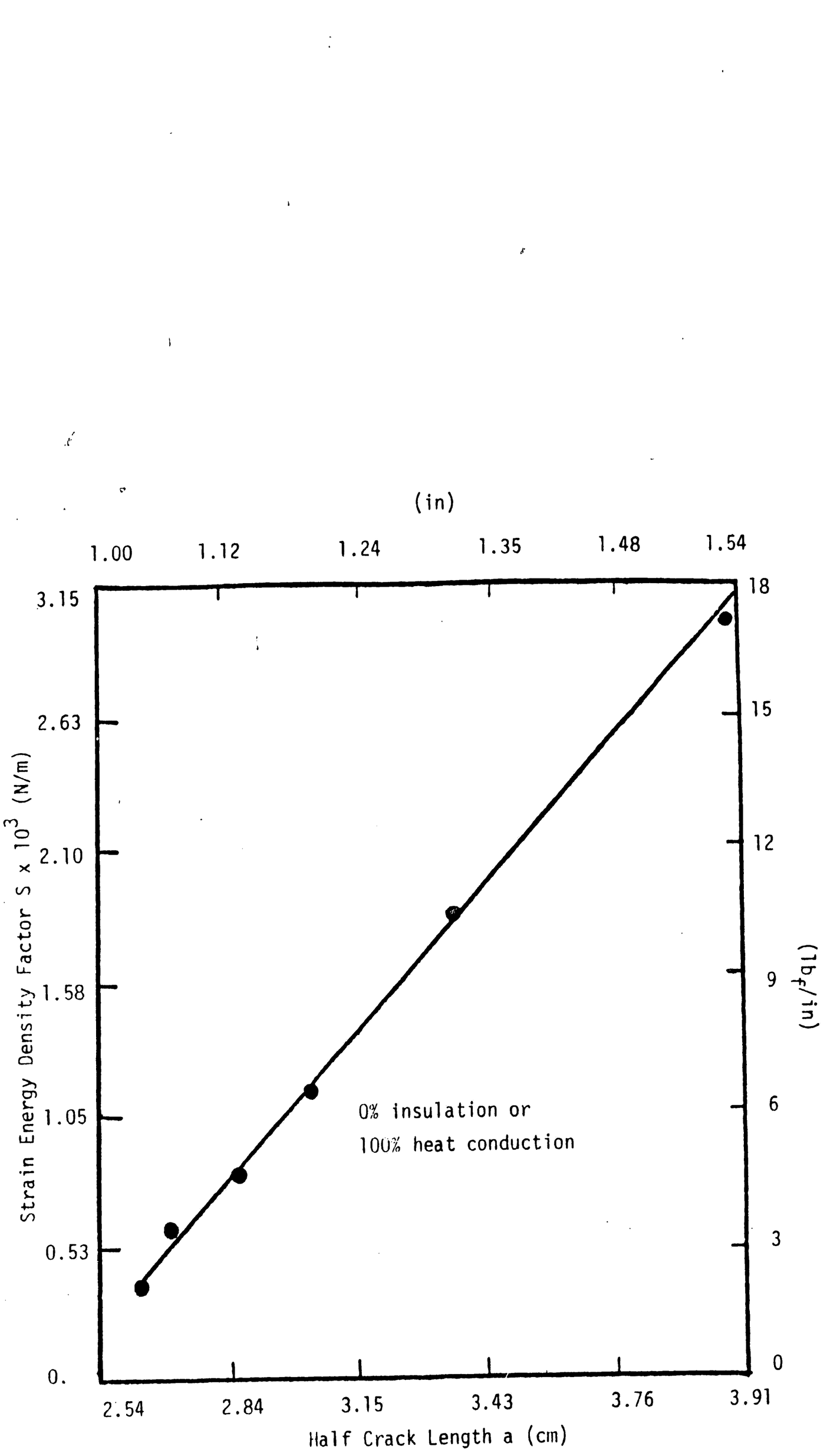

Figure 21 - R-curve for crack with increasing surface temperature.

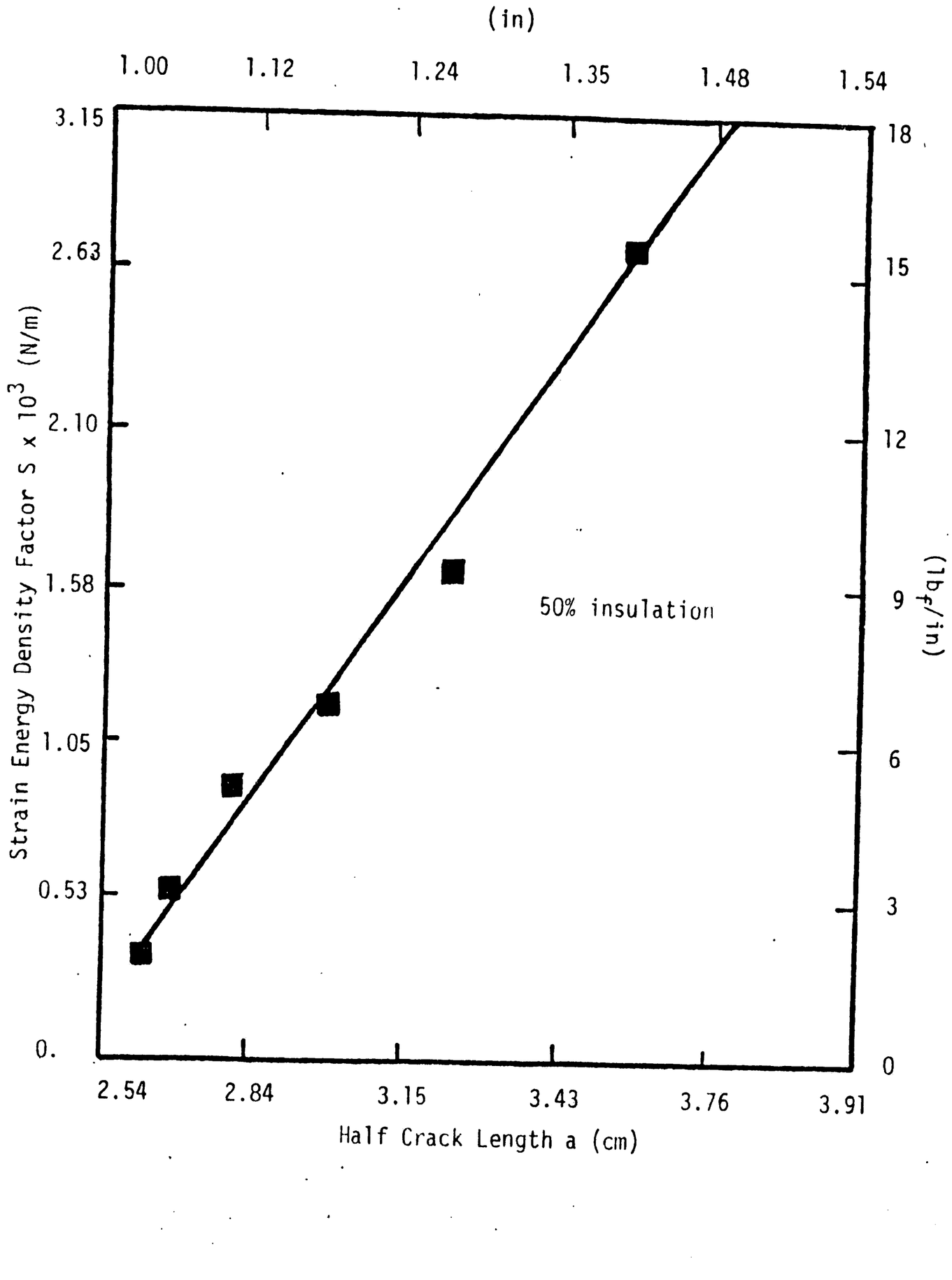

Figure 22 - R-curve for crack with partially insulated surface.

limit, a vertical S versus a line could result. This represents the case of a fully insulated crack with $\partial T/\partial y = 0$ along the entire x-axis. Obviously, no crack growth can occur as the local temperature and stress field would be undisturbed.

CHAPTER 6: CONCLUSIONS AND RECOMMENDATION FOR FUTURE RESEARCH

The problem of heat transfer across a crack treated in this dissertation can be used to model the situation of gas leakage through the cracked wall of a pressure vessel or pipeline. Whether the crack could become unstable or not can be determined from a knowledge of the R-curve that can be made available analytically and verified experimentally in the laboratory. Such information is valuable for establishing design rules and the prevention of catastrophic failure, a situation that should be avoided in service.

Charts such as those in Figure 23 and Figure 24 can also be established as useful information for establishing inspection procedures. They can quickly provide data in the extent of change by crack growth for a given temperature change with different degree of insulation. The ease with which data can be used in design is attributed to the strain energy density failure criterion. Other criteria such as maximum stress, crack opening displacement, path-independent integral, etc., cannot, in general, yield the straight line property for the R-curves.

The present method of solution applies equally well to crack growth accompanied by yielding or permanent deformation. This involves time-dependent energy dissipation and strain rate effects of material response. In particular, crack growth characteristics become highly sensitive to load-time history. The influence of temperature

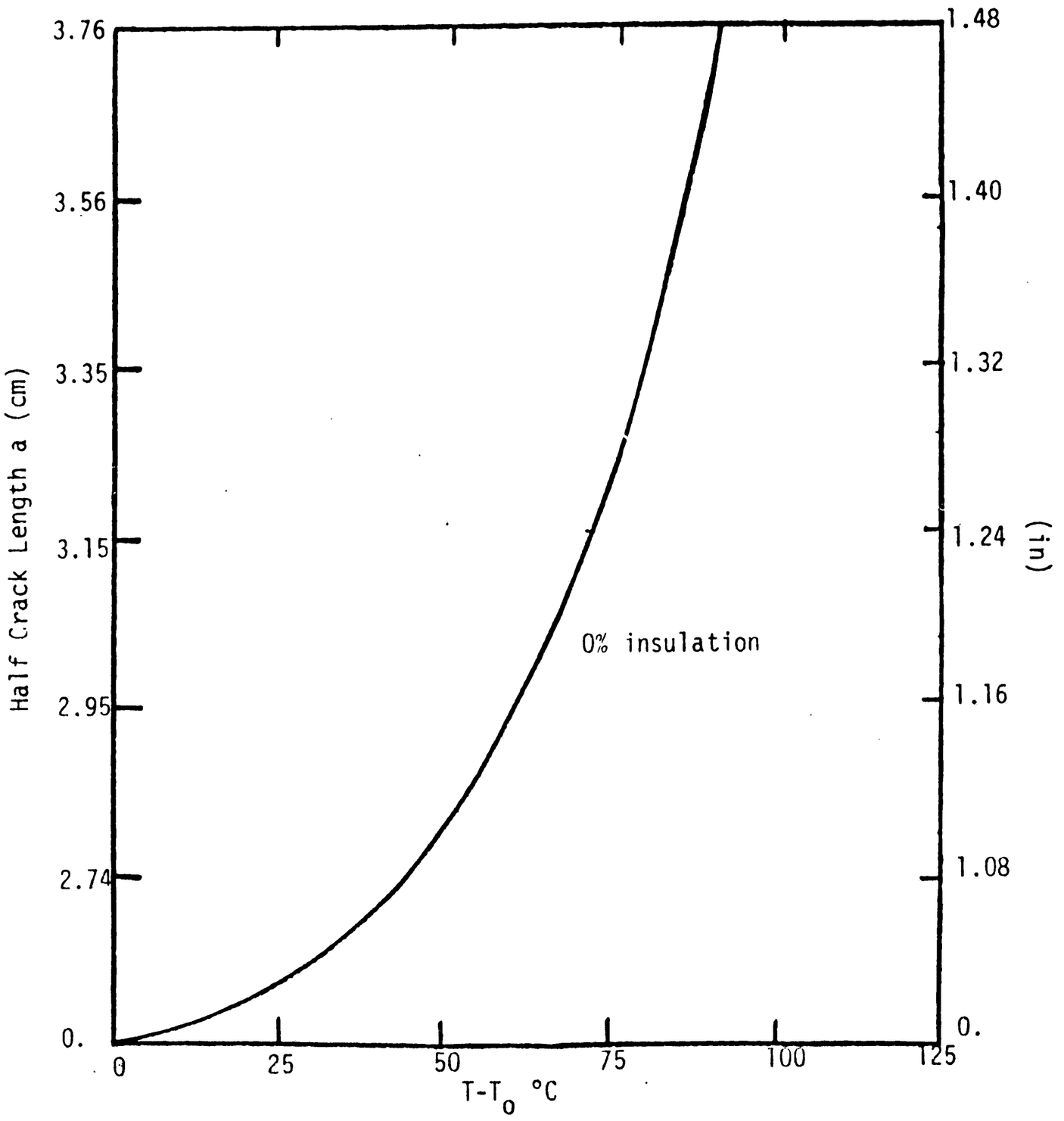

Figure 23 - Crack growth as a function of temperature on crack surface.

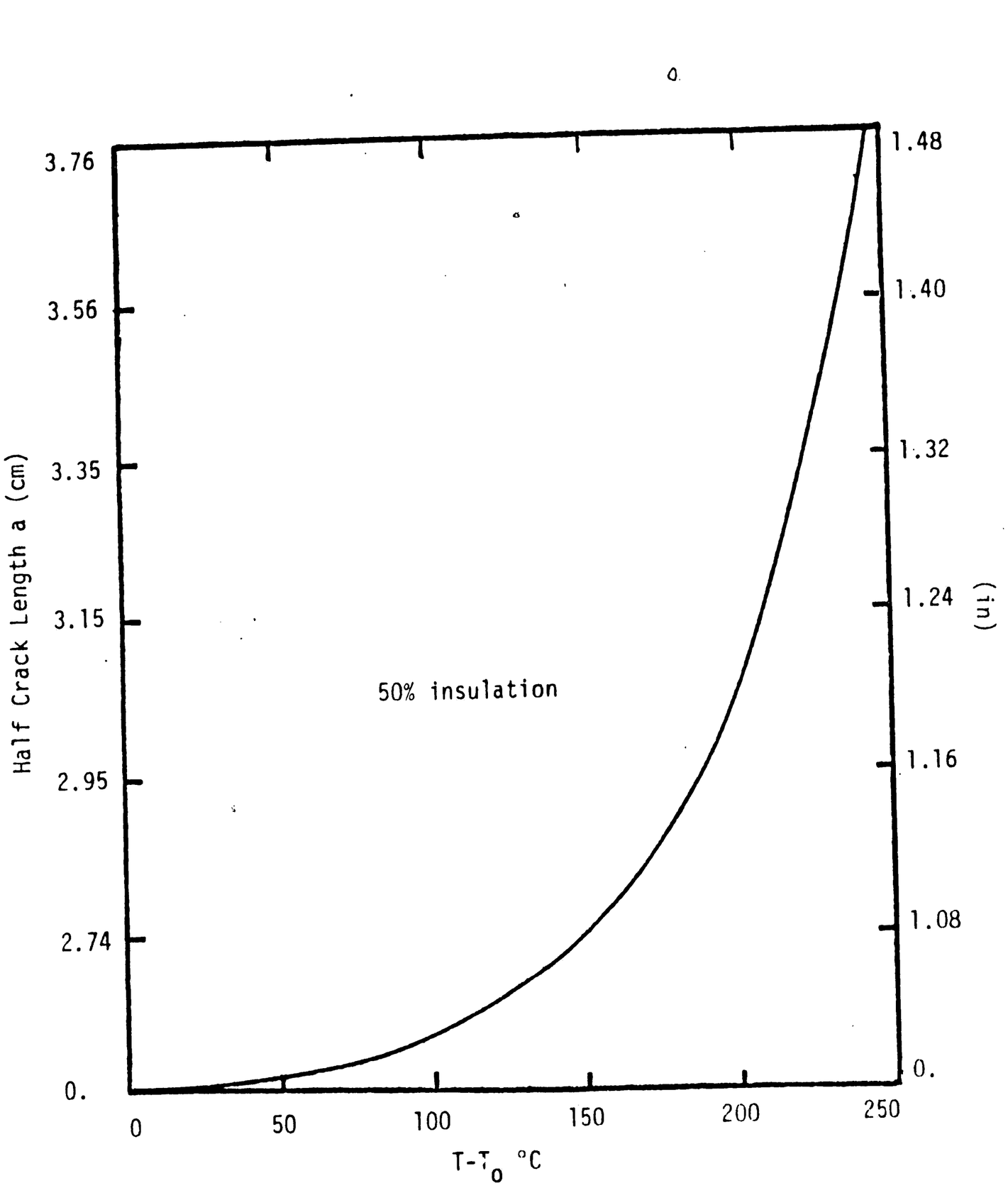

Figure 24 - Crack growth as a function of temperature on panel edge.

changes will interact with material response which, in turn, alters the thermal stress distribution and hence the end results. These effects cannot be adequately described by the conventional theory of plasticity that contains too many simplifying assumptions, one of which is the neglect of the dilatational contribution in the von Mises yield condition. This influence is dominant in the region close to the crack tip and cannot be neglected. Otherwise, large errors can result. One of the most prominent theories that is being developed at the Institute of Fracture and Solid Mechanics at Lehigh University involves the exchange of surface and volume energy. Stress and failure analysis can be performed simultaneously such that the load time history effects can be realistically accounted for providing an unique relation between uniaxial and multiaxial stress states. The application of this theory to problems involving thermal fluctuations will be left for future investigation.

REFERENCES

[1] Mechanics of Fracture, Introductory Chapters, Vol. I to VII, edited by G. C. Sih, Martinus Nijhoff Publishing, The Hague, 1972-1982.

[2] G. C. Sih, Fracture Toughness Concept, ASTM STP 605, pp. 3-15, 1976.

[3] G. C. Sih, "Some Basic Problems in Fracture Mechanics and New Concept", Engineering Fracture Mechanics, 5, pp. 365-371, 1973.

[4] G. C. Sih and B. Macdonald, "Fracture Mechanics Applied to Engineering Problem - Strain Energy Density Fracture Criterion", Engineering Fracture Mechanics, 6, pp. 493-507, 1974.

[5] G. C. Sih, "Strain Energy Density Factor Applied to Mixed Mode Crack Problem", Int. J. of Fracture, 10, 3, pp. 305-321, 1974.

[6] E. E. Gdoutos and G. C. Sih, "Crack Growth Characteristic Influenced by Load Time Record", J. of Theoretical and Applied Fracture Mechanics, Vol. 2, No. 2, pp. 91-103, 1984.

[7] Standard Method of Test for Plane Strain Fracture Toughness of Metallic Media, ASTM E399-74, 1974.

[8] K. H. Huebner, The Finite Element Method for Engineers, John Wiley, 1975.

[9] B. Weiner, Theory of Thermal Stress, John Wiley, 1960.

[10] R. C. Bolton, "Failure Prediction Based on Strain Energy Criterion for Crack and Notch Problems in Thermoelasticity", Unpublished M.S. Thesis, Lehigh University, 1983.

[11] P. D. Hilton, L. N. Gifford, Jr. and O. Lomacky, "Finite Element Fracture Mechanics Analysis of Two-Dimensional and Axisymmetric Elastic and Elastic-Plastic Cracked Structure", Naval Ship Research and Development Center Report 4493, 1975.

VITA

Chich-Kuan Chen, son of Wen-Hsiung Chen and Shei-Ying Chen, was born on March 24, 1960 in Kaohsiung, Taiwan, Republic of China. He graduated from the Provincial Kaohsiung High School in 1978. He attended National Cheng-Kung University in June 1979 and received the Bachelor of Science degree in Mechanical Engineering with honor in June 1983. He was admitted as a graduate student in the Department of Mechanical Engineering and Mechanics of Lehigh University, September 1983.